Table 1. Primer sequences for RT-PCR and ChIP

Primer sequence	Annealing temperature (°C)	Product size (bp)
Quantitative RT-PCR (*p21$^{WAF1/CIP1}$*)		
F: 5′-TGGAGACTCTCAGGGTCGAAA-3′	55	87
R: 5′-GGCGTTTGGAGTGGTAGAAATC-3′		
Quantitative RT-PCR (*ACTB*)		
F: 5′-TCACCGAGCGCGGCT-3′	55	60
R: 5′-TAATGTCACGCACGATTTCCC-3′		
ChIP-PCR (*p21$^{WAF1/CIP1}$* promoter region)		
F: 5′-GGGGCTTTTCTGGAAATTGC-3′	55	116
R: 5′-CTGGCAGGCAAGGATTTACC-3′		
ChIP-PCR (*p21$^{WAF1/CIP1}$* coding region)		
F: 5′-CGCTAATGGCGGGCTG-3′	55	60
R: 5′-CGGTGACAAAGTCGAAGTTCC-3′		
ChIP-PCR (*ACTB* 5′ upstream region)		
F: 5′-CCCACCCGGTCTTGTGTG-3′	55	72
R: 5′-GGGAAGACCCTGTCCTTGTCA-3′		

and sequences of primers, and annealing temperatures, are shown in Table 1 and Figure 1A. PCR was performed with the SYBR Green PCR Core Reagents Kit (Applied Biosystems, Tokyo, Japan). Real-time detection of the emission intensity of SYBR Green bound to double-stranded DNAs was done with the ABI PRISM 7700 Sequence Detection System (Applied Biosystems). The relative histone acetylation level was determined from the threshold cycles for the promoter or coding region of the *p21$^{WAF1/CIP1}$* gene and the 5′ region of the *ACTB* gene. Reference samples (genomic DNA from MKN-1 cells) were included on each assay plate to verify plate-to-plate consistency. Plates were normalized to each other with these reference samples. The PCR amplification was performed in 96-well optical trays with caps according to the manufacturer's instructions. Quantitative PCRs were performed in triplicate for each sample primer set, and the mean of the three experiments was calculated as the relative quantification value. At the end of 40 PCR cycles, reaction products were separated electrophoretically on 8% non-denaturing polyacrylamide gels for visual confirmation of PCR products.

Quantitative reverse transcription (RT)-PCR analysis of GC tissues

Total RNA was extracted with an RNeasy Mini Kit (QIAGEN, Hilden, Germany), and 1 μg of total RNA was converted to cDNA with a First Strand cDNA Synthesis Kit (Amersham Pharmacia Biotech, Uppsala, Sweden). To analyse expression of the *p21$^{WAF1/CIP1}$* gene in GC tissue specimens, real-time RT-PCR was performed as described previously [29]. Primer sequences and annealing temperatures are shown in Table 1. PCR was performed with the SYBR Green PCR Core Reagents Kit (Applied Biosystems). Reference samples (MKN-1) were included on each assay plate to verify plate-to-plate consistency.

Western blot analysis of GC cell lines

Preparation of whole cell lysates from GC cell lines and western blotting were performed as described previously [30]. Protein concentrations were determined by Bradford protein assay (Bio-Rad, Hercules, CA, USA) with bovine serum albumin (BSA) used as the standard. Lysates (20 μg) were solubilized in Laemmli's sample buffer by boiling and then subjected to 10% SDS-PAGE followed by electrotransfer onto a nitrocellulose filter. Anti-p21$^{WAF1/CIP1}$ monoclonal antibody was purchased from PharMingen (San Diego, CA, USA). Peroxidase-conjugated anti-mouse IgG was used in the secondary reaction. The immunocomplex was visualized with an ECL Western Blot Detection System (Amersham Pharmacia Biotech). The quality and amount of each protein sample on the gel were confirmed by detection with anti-beta-actin antibody (Sigma). Autoradiographic signal intensities of the p21$^{WAF1/CIP1}$ bands on western blots were determined by densitometric scanning and normalization of these signals to those of the internal control (beta-actin).

DNA extraction and p53 mutation analysis

To examine mutations in the *p53* gene, genomic DNAs were extracted from GC specimens with a genomic DNA purification kit (Promega, Madison, WI, USA). Exons 5–8 of the *p53* gene were amplified by PCR with ten sets of primers as described previously [31]. The PCR products were purified and sequenced directly with the ABI Prism Dye Terminator Cycle Sequencing Kit (Applied Biosystems) and an ABI Prism 310 DNA Sequencer (Applied Biosystems).

Statistical methods

Differences were analysed statistically by Fisher's exact and Mann–Whitney *U*-tests. *p* values less than 0.05 were considered statistically significant.

Results

Histone acetylation status in GC tissues

To examine the *in vivo* status of histone acetylation and expression of $p21^{WAF1/CIP1}$, $p21^{WAF1/CIP1}$ mRNA levels were measured by quantitative RT-PCR (Figure 1B) and acetylation of histones H3 and H4 by ChIP in 29 GC specimens (Figure 1C). The ratio of histone acetylation levels in GC specimens relative to those in non-neoplastic mucosae (T/N) was calculated. A T/N of less than 0.5 was considered to represent hypoacetylation, and a T/N of greater than 2.0 was considered to represent hyperacetylation. Hypoacetylation of histone H3 in the promoter

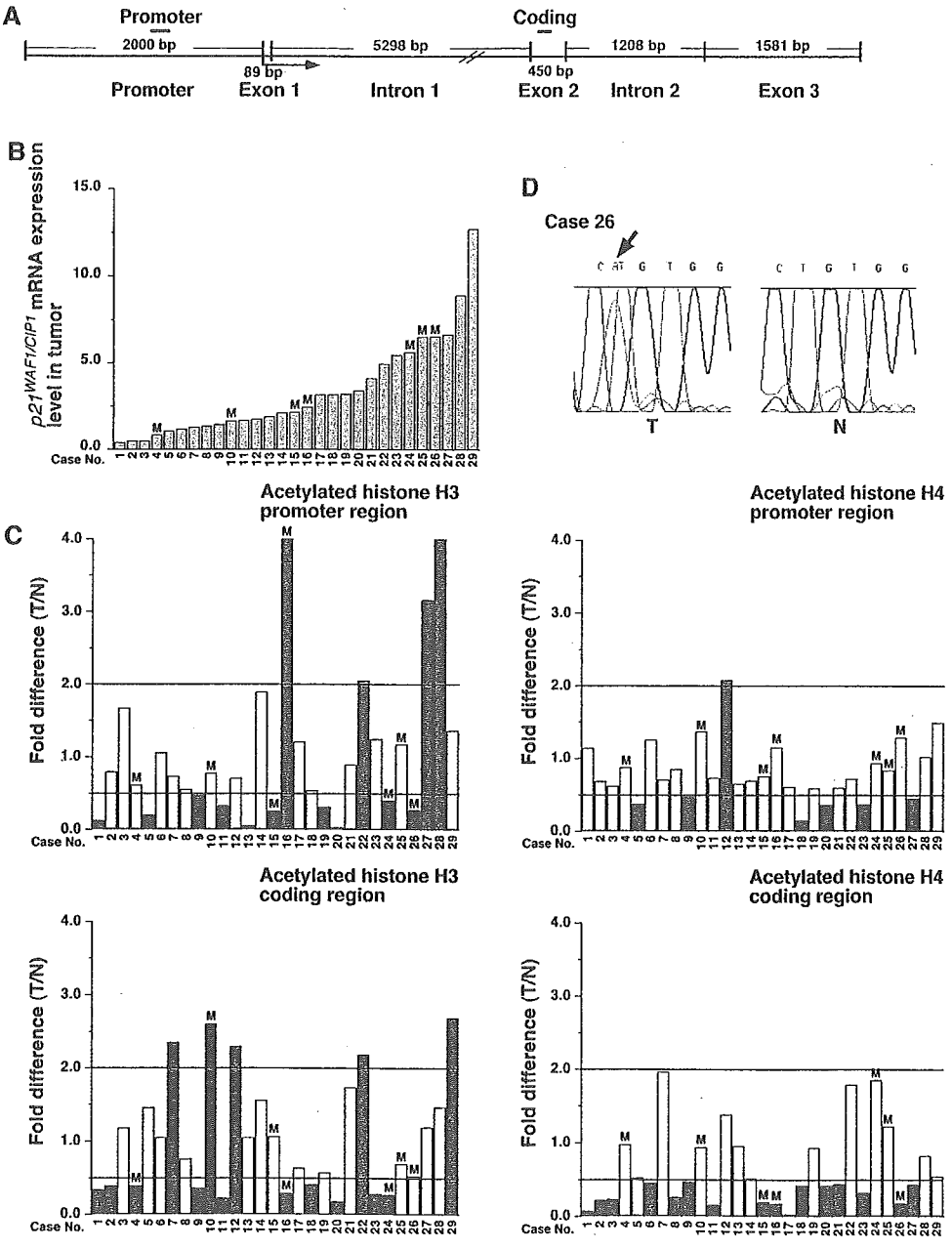

Figure 1. Expression and acetylation of the $p21^{WAF1/CIP1}$ gene and p53 mutation status in GC tissues. (A) Schematic representation of the human $p21^{WAF1/CIP1}$ gene. Positions of the primer pairs used in the present study are indicated as black bars (Promoter and Coding). (B) Quantitative RT-PCR analysis of $p21^{WAF1/CIP1}$. Units are arbitrary and we calculated $p21^{WAF1/CIP1}$ mRNA levels by standardization against 1 μg of total RNA from MKN-1 cells, which was taken as 1.0. The 29 GC tissues are sorted by increasing $p21^{WAF1/CIP1}$ expression. M indicates specimens carrying p53 mutations. (C) ChIP analysis of histones H3 and H4 in the $p21^{WAF1/CIP1}$ promoter and coding regions in 29 GC tissues. Fold change indicates the ratio of $p21^{WAF1/CIP1}$ acetylation level in GC to that in corresponding non-neoplastic mucosa (T/N). We considered a T/N < 0.5 (red bars) to indicate hypoacetylation and a T/N > 2.0 (green bars) to indicate hyperacetylation. (D) Sequencing analysis of the p53 gene (case 26, exon 5). There is a mutation in codon 145 (CTG to CAG, arrow)

and coding regions of $p21^{WAF1/CIP1}$ was observed in 10 (34.5%) and 10 (34.5%) of 29 specimens, respectively. Hypoacetylation of histone H4 in the promoter and coding regions was found in 6 (20.7%) and 16 (55.2%) of 29 specimens, respectively. $p21^{WAF1/CIP1}$ mRNA levels in tumour tissues with histone H3 hypoacetylation in the promoter region were significantly lower than those in specimens with histone H3 hyperacetylation ($p = 0.047$; Mann–Whitney U-test), whereas $p21^{WAF1/CIP1}$ levels in tumour tissues were not associated with histone H3 acetylation status in the coding region ($p = 0.540$; Mann–Whitney U-test, Table 2). No association was found between $p21^{WAF1/CIP1}$ levels and histone H4 acetylation status in either the promoter or the coding regions of $p21^{WAF1/CIP1}$

The correlation was then examined between $p53$ mutation status and $p21^{WAF1/CIP1}$ mRNA expression, and histone acetylation. Representative results of $p53$ sequencing analysis are shown in Figure 1D, and the results of $p53$ mutation analyses are summarized in Table 3. $p53$ gene mutation was detected in 10 (34.5%) of 29 specimens. Of the ten mutations, seven were missense mutations and three were silent mutations. The seven missense mutations were analysed further. The level of $p21^{WAF1/CIP1}$ expression was not associated with $p53$ mutation status ($p = 0.460$; Mann–Whitney U-test), and $p53$ mutation status did not correlate with histone acetylation status (data not shown). Histone acetylation status was not associated with T grade (depth of tumour invasion), N grade (degree of lymph node metastasis), tumour stage, or histological type (data not shown).

TSA induced $p21^{WAF1/CIP1}$ expression and histone H3 hyperacetylation

To confirm the correlation between reduced $p21^{WAF1/CIP1}$ expression and hypoacetylation of histones, $p21^{WAF1/CIP1}$ expression and histone acetylation status were examined in eight GC cell lines. Levels of p21$^{WAF1/CIP1}$ protein were measured by western blot analysis (Figure 2A). Levels of p21$^{WAF1/CIP1}$ in GC cell lines were classified into three groups. MKN-45 and MKN-74 showed high levels of expression; MKN-28, TMK-1, and HSC-39 showed intermediate expression; and MKN-1, MKN-7, and KATO-III showed low expression. One cell line was selected from each group (MKN-74, MKN-28, and KATO-III) for further analysis. The effects of TSA and Aza-dC on p21$^{WAF1/CIP1}$ protein expression were examined by western blot analysis (Figure 2B). MKN-28 (mutant-type p53), MKN-74 (wild-type p53), and KATO-III (p53 null) cells were cultured with or without TSA for 24 h or Aza-dC for 5 days. Treatment with TSA increased the p21$^{WAF1/CIP1}$ protein levels in all three cell lines, whereas the p53 protein levels did not change. TSA induced 5.2-fold and 6.1-fold increases in p21$^{WAF1/CIP1}$ protein levels in MKN-28 and KATO-III cells, respectively, whereas TSA yielded only a 1.4-fold increase in p21$^{WAF1/CIP1}$ protein levels in MKN-74 cells. Treatment with Aza-dC had no effect on p21$^{WAF1/CIP1}$ protein expression in any of the cell lines (Figure 2B). ChIP assay was carried out to investigate acetylation of histones H3 and H4 associated with the $p21^{WAF1/CIP1}$ gene (Figure 2C). TSA increased acetylation of histone H3 in both the promoter and coding regions of $p21^{WAF1/CIP1}$ in both MKN-28 and KATO-III cells. Histone H4 acetylation in the $p21^{WAF1/CIP1}$ promoter region in MKN-28 cells was increased slightly in response to TSA, whereas that in KATO-III cells was increased significantly. Histone H4 acetylation in the coding region was increased markedly by TSA in both MKN-28 and KATO-III

Table 3. Summary of $p53$ mutations

Case No	Location	Codon	Sequence change	Amino acid
4	Exon 7	245	GGC to GTC	Gly to Val
5	Exon 5a	129	GCC to GCT	Ala to Ala
10	Exon 5b	160	ATG to ATA	Met to Ile
15	Exon 7	251	ATC to AAC	Ile to Asn
16	Exon 5b	160	ATG to ACG	Met to Thr
18	Exon 5a	129	GCC to GCT	Ala to Ala
21	Exon 7	240	AGT to AGC	Ser to Ser
24	Exon 5b	173	GTG to GCG	Val to Ala
25	Exon 5a	128	CCT to ACT	Pro to Thr
26	Exon 5a	145	CTG to CAG	Leu to Gln

Table 2. Association between $p21^{WAF1/CIP1}$ mRNA levels and histone acetylation status

		No of cases	$p21^{WAF1/CIP1}$ mRNA level (mean ± SE)*	p value†
Histone H3 acetylation status in promoter region	Hypo	10	2.71 ± 0.62	0.047
	Hyper	4	5.71 ± 1.36	
Histone H3 acetylation status in coding region	Hypo	10	2.47 ± 0.60	0.540
	Hyper	5	4.43 ± 2.16	
Histone H4 acetylation status in promoter region	Hypo	6	3.50 ± 0.89	0.617
	Hyper	1	1.71	
Histone H4 acetylation status in coding region	Hypo	16	2.73 ± 0.511	—
	Hyper	0	—	

* The units are arbitrary and we calculated the $p21^{WAF1/CIP}$ mRNA expression level by standardization against 1 μg of total RNA from MKN-1 GC cells taken as 1.0. SE = standard error.
† Mann–Whitney U-test. Hypo = hypoacetylation; Hyper = hyperacetylation.

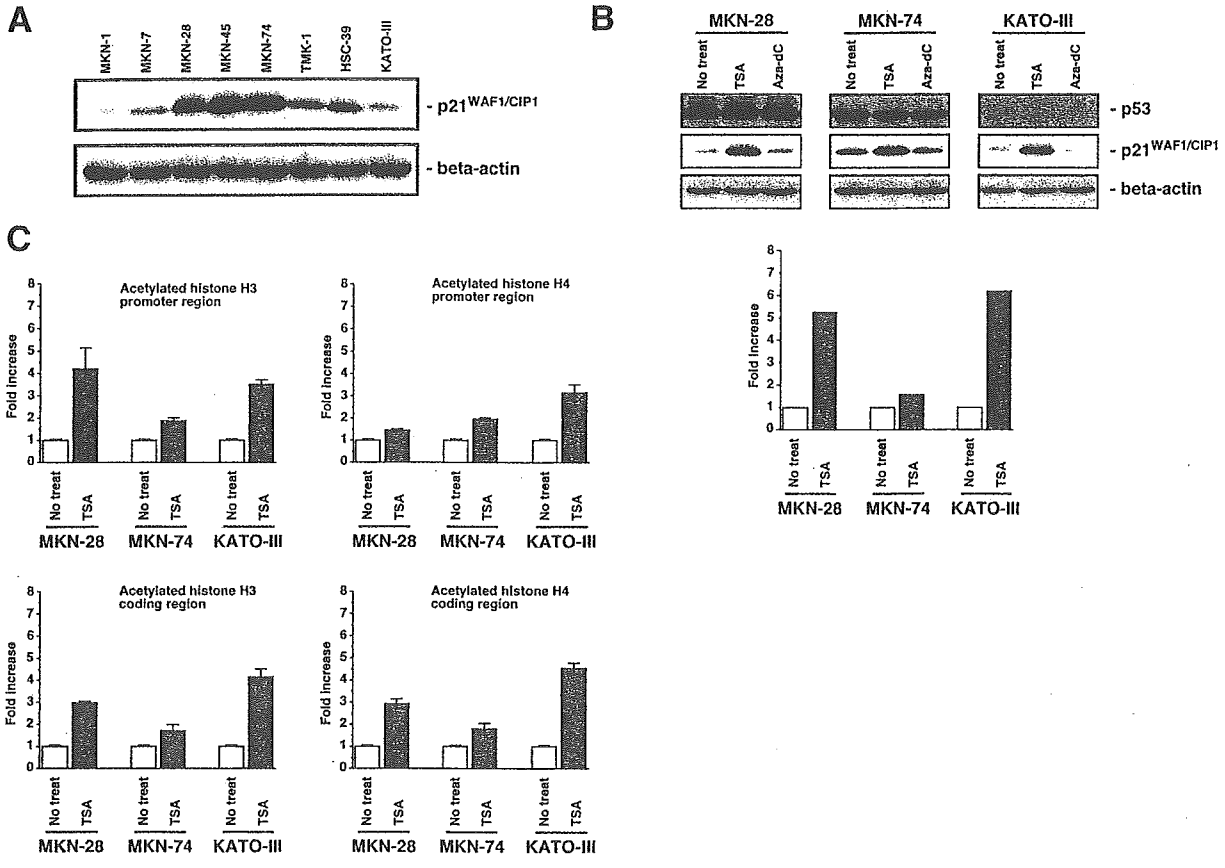

Figure 2. p21$^{WAF1/CIP1}$ protein expression and histone acetylation status in GC cell lines. (A) Western blot analysis of p21$^{WAF1/CIP1}$ in eight GC cell lines. MKN-45 and MKN-74 cells showed high expression. MKN-28, TMK-1, and HSC-39 cells showed intermediate expression. MKN-1, MKN-7, and KATO-III cells showed low expression. (B) Western blot analysis of p53 and p21$^{WAF1/CIP1}$ in three GC cell lines cultured with or without TSA for 24 h or Aza-dC for 5 days. In all three cell lines, TSA treatment induced p21$^{WAF1/CIP1}$ expression, whereas Aza-dC treatment did not. The relative p21$^{WAF1/CIP1}$ band intensity normalized to that of beta-actin is indicated in the lower panel. (C) ChIP analyses of the relative levels of histones H3 and H4 in the *p21*$^{WAF1/CIP1}$ promoter and coding regions in three GC cell lines. The value is the mean of three independent ChIP experiments. Error bars indicate the standard error (SE) of the mean. Note that acetylation of histone H4 in the promoter region does not increase significantly after TSA treatment in MKN-28 cells

cells. In MKN-74 cells, acetylation of histones H3 and H4 in both the promoter and coding regions was increased approximately 2.0-fold.

Inhibition of p53-induced hypoacetylation of histone H4

To investigate the effect of p53 on p21$^{WAF1/CIP1}$ protein levels, the MKN-74 cell line was stably transfected with a vector expressing a dominant-negative mutant of p53, and p21$^{WAF1/CIP1}$ protein levels were determined by western blot analysis (Figure 3A). p21$^{WAF1/CIP1}$ levels in p53 mutant cells were less than half those in wild-type cells. ChIP was also used to analyse histone acetylation levels (Figure 3B). Histone H4 acetylation levels in both the promoter and coding regions of cells expressing dominant-negative p53 were less than half those in cells expressing wild-type p53, whereas histone H3 acetylation levels in both the promoter and coding regions were reduced slightly (approximately 20%) in cells expressing dominant-negative p53.

Discussion

A variety of genetic and epigenetic alterations are associated with GC. Histone acetylation and DNA methylation appear to play important roles in transcriptional regulation; however, little is known about changes in histone acetylation in human cancers such as GC. In the present study, we investigated the histone acetylation status in regions of the *p21*$^{WAF1/CIP1}$ gene in GC tissues and GC cell lines.

We found that histones H3 and H4 in both the promoter and coding regions are hypoacetylated in GC tissues. *p21*$^{WAF1/CIP1}$ mRNA levels are associated with histone H3 acetylation status in the promoter region, suggesting that nucleosome conformation was altered due to histone H3 hypoacetylation and that access of transcriptional regulatory proteins to chromatin might be reduced in GC tissues. It is possible that histone hypoacetylation and reduced *p21*$^{WAF1/CIP1}$ expression were the result of the p53 mutation because previous studies have shown an interaction between p53 and chromatin-modifying enzymes.

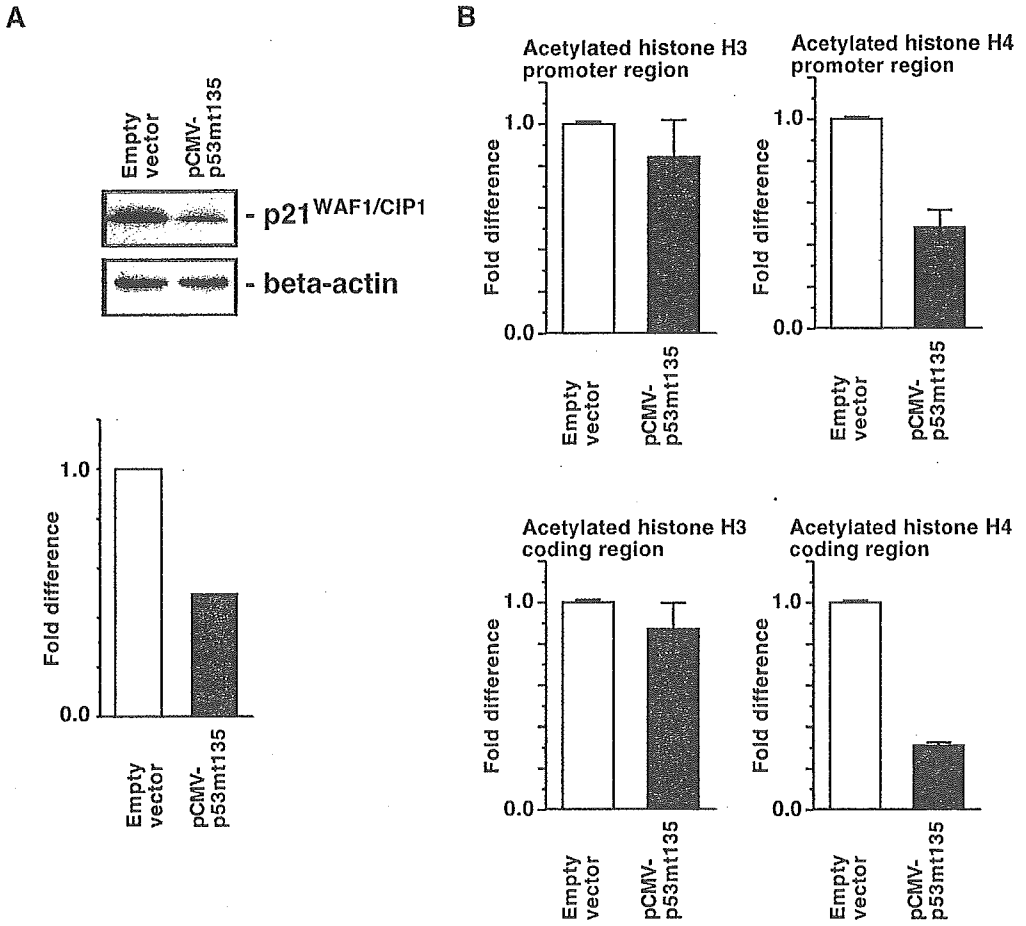

Figure 3. Effect of a dominant-negative (DN) mutant of p53 in MKN-74 cells. (A) Western blot analysis of p21$^{WAF1/CIP1}$ (upper panel). Expression of DN p53 reduced p21$^{WAF1/CIP1}$ expression. p21$^{WAF1/CIP1}$ band intensity normalized against beta-actin is indicated in the lower panel. (B) ChIP analyses of relative levels of histones H3 and H4 in the $p21^{WAF1/CIP1}$ promoter and coding regions. The value is the mean of three independent ChIP experiments. Error bars are the standard error (SE) of the mean. Note that expression of DN p53 reduced acetylation of histone H4 in both the promoter and coding regions of $p21^{WAF1/CIP1}$

Several acetyltransferases act as p53 co-activators and regulate the transcriptional activity of p53 [32,33]. In addition, we showed that a dominant-negative p53 mutant affects histone acetylation in MKN-74 cells. However, in our study, *p53* mutation status correlated with neither histone acetylation status nor $p21^{WAF1/CIP1}$ expression in GC tissues. Because several factors, such as transforming growth factor beta and nerve growth factor, have been reported to activate transcription of $p21^{WAF1/CIP1}$ [34], we cannot rule out the possibility that they cause hypoacetylation of histones in the $p21^{WAF1/CIP1}$ promoter. However, altered hypoacetylation of histone H3 in GC tissues does not appear to be due to a mutant form of p53 because p53 appears to affect acetylation of only histone H4 [35]. We also showed that expression of a dominant-negative p53 mutant suppresses p21$^{WAF1/CIP1}$ expression and that acetylation of histone H4 in the promoter is reduced significantly. Taken together, our data indicate that aberrant hypoacetylation of histones in the $p21^{WAF1/CIP1}$ promoter occurs in GC.

We found no association between $p21^{WAF1/CIP1}$ expression and histone H4 acetylation status in the $p21^{WAF1/CIP1}$ promoter in GC tissues and MKN-28 cells. In MDA-MB-435 cells, trapoxin (TPX), an HDAC inhibitor, significantly increases acetylation of histone H3 in the $p21^{WAF1/CIP1}$ promoter, whereas TPX does not significantly affect acetylation of histone H4 [36]. Similar results have been reported in HDAC1-null embryonic stem cells [37]. These results indicate that hyperacetylation of histone H4 in the $p21^{WAF1/CIP1}$ promoter region is not an absolute requirement for $p21^{WAF1/CIP1}$ expression.

HDAC inhibition appears to influence histone H3 hyperacetylation, whereas p53 appears to affect histone H4 hyperacetylation. Our present results also suggest that acetylated histones H3 and H4 have distinct roles. Distinct roles for acetylation of histones H3 and H4 have been reported in yeast [38]. Although a number of studies have shown induction of $p21^{WAF1/CIP1}$ by HDAC inhibitors, p53, and Sp1 [33,35,39], the significance of distinct roles for acetylation of histones H3 and H4 is not clear in human cancer cells. Further studies may reveal the functional significance of the acetylation of histones H3 and H4.

We also investigated the histone acetylation status in the coding region of $p21^{WAF1/CIP1}$. In GC cell lines, expression of $p21^{WAF1/CIP1}$ protein is associated with acetylation of histones H3 and H4 in the $p21^{WAF1/CIP1}$ coding region. This is consistent with the idea that transcript elongation and histone acetylation are needed to form and maintain, respectively, the relaxed structure of transcribing nucleosomes [40]. In contrast to our findings in cell lines, we found no association between $p21^{WAF1/CIP1}$ expression and histone acetylation status in the coding region in GC tissues. However, our data do show that histone H4 in the $p21^{WAF1/CIP1}$ coding region is frequently hypoacetylated in GC tissues. Although there have been many studies of promoter histone acetylation, the function of histone acetylation in coding regions is poorly understood. The significance of histone H4 hypoacetylation in the coding region of $p21^{WAF1/CIP1}$ remains unclear, but it is possible that it contributes to a change in nucleosome conformation. Further studies are needed to elucidate the function of histone acetylation in coding regions.

In conclusion, we have shown that histones H3 and H4 in both the promoter and coding regions of the $p21^{WAF1/CIP1}$ gene are frequently hypoacetylated in GC tissues. Hypoacetylation of histone H3 in the promoter region is associated with reduced expression of $p21^{WAF1/CIP1}$ in a p53-independent manner. Clinical trials of HDAC inhibitors as cancer therapeutics are underway [41,42]. Although we did not investigate the anti-tumour activity of $p21^{WAF1/CIP1}$ and HDAC inhibitors in GC, our data provide supporting evidence for the idea that inhibition of HDAC may be an effective therapy for patients with GC.

Acknowledgements

We thank Mr K Tominaga and Ms Y Kaneko for excellent technical assistance and advice. This work was carried out with the kind cooperation of the Research Center for Molecular Medicine (RCMM), Faculty of Medicine, Hiroshima University. This work was supported, in part, by Grants-in-Aid for Cancer Research from the Ministry of Education, Culture, Science, Sports, and Technology of Japan; and from the Ministry of Health, Labor, and Welfare of Japan.

References

1. Yasui W, Oue N, Ono S, Mitani Y, Ito R, Nakayama H. Histone acetylation and gastrointestinal carcinogenesis. *Ann N Y Acad Sci* 2003; **983**: 220–231.
2. Oue N, Hamai Y, Mitani Y, *et al.* Gene expression profile of gastric carcinoma: identification of genes and tags potentially involved in invasion, metastasis, and carcinogenesis by serial analysis of gene expression. *Cancer Res* 2004; **64**: 2397–2405.
3. Yasui W, Akama Y, Kuniyasu H, *et al.* Expression of cyclin-dependent kinase inhibitor p21WAF1/CIP1 in non-neoplastic mucosa and neoplasia of the stomach: relationship with p53 status and proliferative activity. *J Pathol* 1996; **180**: 122–128.
4. el-Deiry WS, Tokino T, Velculescu VE, *et al.* WAF1, a potential mediator of p53 tumor suppression. *Cell* 1993; **75**: 817–825.
5. Harper JW, Adami GR, Wei N, Keyomarsi K, Elledge SJ. The p21 Cdk-interacting protein Cip1 is a potent inhibitor of G1 cyclin-dependent kinases. *Cell* 1993; **75**: 805–816.
6. Noda A, Ning Y, Venable SF, Pereira-Smith OM, Smith JR. Cloning of senescent cell-derived inhibitors of DNA synthesis using an expression screen. *Exp Cell Res* 1994; **211**: 90–98.
7. Naka K, Yokozaki H, Domen T, *et al.* Growth inhibition of cultured human gastric cancer cells by 9-*cis*-retinoic acid with induction of cdk inhibitor Waf1/Cip1/Sdi1/p21 protein. *Differentiation* 1997; **61**: 313–320.
8. Naka K, Yokozaki H, Yasui W, Tahara H, Tahara E. Effect of antisense human telomerase RNA transfection on the growth of human gastric cancer cell lines. *Biochem Biophys Res Commun* 1999; **255**: 753–758.
9. Jones PA, Baylin SB. The fundamental role of epigenetic events in cancer. *Nature Rev Genet* 2002; **3**: 415–428.
10. Kass SU, Pruss D, Wolffe AP. How does DNA methylation repress transcription? *Trends Genet* 1997; **13**: 444–449.
11. Oue N, Motoshita J, Yokozaki H, *et al.* Distinct promoter hypermethylation of p16INK4a, CDH1, and RAR-beta in intestinal, diffuse-adherent, and diffuse-scattered type gastric carcinomas. *J Pathol* 2002; **198**: 55–59.
12. Oue N, Oshimo Y, Nakayama H, *et al.* DNA methylation of multiple genes in gastric carcinoma: association with histological type and CpG island methylator phenotype. *Cancer Sci* 2003; **94**: 901–905.
13. Roman-Gomez J, Castillejo JA, Jimenez A, *et al.* 5′ CpG island hypermethylation is associated with transcriptional silencing of the p21(CIP1/WAF1/SDI1) gene and confers poor prognosis in acute lymphoblastic leukemia. *Blood* 2002; **99**: 2291–2296.
14. Shin JY, Kim HS, Park J, Park JB, Lee JY. Mechanism for inactivation of the KIP family cyclin-dependent kinase inhibitor genes in gastric cancer cells. *Cancer Res* 2000; **60**: 262–265.
15. Grunstein M. Histone acetylation in chromatin structure and transcription. *Nature* 1997; **389**: 349–352.
16. Eberharter A, Becker PB. Histone acetylation: a switch between repressive and permissive chromatin. Second in review series on chromatin dynamics. *EMBO Rep* 2002; **3**: 224–229.
17. Urnov FD, Wolffe AP. Chromatin remodeling and transcriptional activation: the cast (in order of appearance). *Oncogene* 2001; **20**: 2991–3006.
18. Luger K, Richmond TJ. The histone tails of the nucleosome. *Curr Opin Genet Dev* 1998; **8**: 140–146.
19. Luger K, Mader AW, Richmond RK, Sargent DF, Richmond TJ. Crystal structure of the nucleosome core particle at 2.8 Å resolution. *Nature* 1997; **389**: 251–260.
20. Richon VM, Sandhoff TW, Rifkind RA, Marks PA. Histone deacetylase inhibitor selectively induces p21WAF1 expression and gene-associated histone acetylation. *Proc Natl Acad Sci U S A* 2000; **97**: 10014–10019.
21. Takakura M, Kyo S, Sowa Y, *et al.* Telomerase activation by histone deacetylase inhibitor in normal cells. *Nucleic Acids Res* 2001; **29**: 3006–3011.
22. Suzuki T, Yokozaki H, Kuniyasu H, *et al.* Effect of trichostatin A on cell growth and expression of cell cycle- and apoptosis-related molecules in human gastric and oral carcinoma cell lines. *Int J Cancer* 2000; **88**: 992–997.
23. Kristjuhan A, Walker J, Suka N, *et al.* Transcriptional inhibition of genes with severe histone h3 hypoacetylation in the coding region. *Mol Cell* 2002; **10**: 925–933.
24. Lauren P. The two histological main types of gastric carcinoma. Diffuse and so-called intestinal type carcinoma: an attempt at histological classification. *Acta Pathol Microbiol Scand* 1965; **64**: 31–49.
25. Sobin LH, Wittekind CH (eds). *TNM Classification of Malignant Tumors* (5th edn). Wiley-Liss: New York, 1997; 59–62.
26. Ochiai A, Yasui W, Tahara E. Growth-promoting effect of gastrin on human gastric carcinoma cell line TMK-1. *Jpn J Cancer Res* 1985; **76**: 1064–1071.
27. Yanagihara K, Seyama T, Tsumuraya M, Kamada N, Yokoro K. Establishment and characterization of human signet ring cell

gastric carcinoma cell lines with amplification of the c-myc oncogene. *Cancer Res* 1991; **51**: 381–386.
28. Ferreira R, Naguibneva I, Mathieu M, *et al.* Cell cycle-dependent recruitment of HDAC-1 correlates with deacetylation of histone H4 on an Rb-E2F target promoter. *EMBO Rep* 2001; **2**: 794–799.
29. Kondo T, Oue N, Yoshida K, *et al.* Expression of POT1 is associated with tumor stage and telomere length in gastric carcinoma. *Cancer Res* 2004; **64**: 523–529.
30. Yasui W, Ayhan A, Kitadai Y, *et al.* Increased expression of p34cdc2 and its kinase activity in human gastric and colonic carcinomas. *Int J Cancer* 1993; **53**: 36–41.
31. Oue N, Shigeishi H, Kuniyasu H, *et al.* Promoter hypermethylation of MGMT is associated with protein loss in gastric carcinoma. *Int J Cancer* 2001; **93**: 805–809.
32. Avantaggiati ML, Ogryzko V, Gardner K, Giordano A, Levine AS, Kelly K. Recruitment of p300/CBP in p53-dependent signal pathways. *Cell* 1997; **89**: 1175–1184.
33. Espinosa JM, Emerson BM. Transcriptional regulation by p53 through intrinsic DNA/chromatin binding and site-directed cofactor recruitment. *Mol Cell* 2001; **8**: 57–69.
34. Gartel AL, Tyner AL. Transcriptional regulation of the p21(WAF1/CIP1) gene. *Exp Cell Res* 1999; **246**: 280–289.
35. Lagger G, Doetzlhofer A, Schuettengruber B, *et al.* The tumor suppressor p53 and histone deacetylase 1 are antagonistic regulators of the cyclin-dependent kinase inhibitor p21/WAF1/CIP1 gene. *Mol Cell Biol* 2003; **23**: 2669–2679.
36. Sambucetti LC, Fischer DD, Zabludoff S, *et al.* Histone deacetylase inhibition selectively alters the activity and expression of cell cycle proteins leading to specific chromatin acetylation and antiproliferative effects. *J Biol Chem* 1999; **274**: 34 940–34 947.
37. Lagger G, O'Carroll D, Rembold M, *et al.* Essential function of histone deacetylase 1 in proliferation control and CDK inhibitor repression. *EMBO J* 2002; **21**: 2672–2681.
38. Wan JS, Mann RK, Grunstein M. Yeast histone H3 and H4 N termini function through different GAL1 regulatory elements to repress and activate transcription. *Proc Natl Acad Sci U S A* 1995; **92**: 5664–5668.
39. Sowa Y, Orita T, Hiranabe-Minamikawa S, *et al.* Histone deacetylase inhibitor activates the p21/WAF1/Cip1 gene promoter through the Sp1 sites. *Ann N Y Acad Sci* 1999; **886**: 195–199.
40. Walia H, Chen HY, Sun JM, Holth LT, Davie Jr. Histone acetylation is required to maintain the unfolded nucleosome structure associated with transcribing DNA. *J Biol Chem* 1998; **273**: 14 516–14 522.
41. Kelly WK, Richon VM, O'Connor O, *et al.* Phase I clinical trial of histone deacetylase inhibitor: suberoylanilide hydroxamic acid administered intravenously. *Clin Cancer Res* 2003; **9**: 3578–3588.
42. Carducci MA, Gilbert J, Bowling MK, *et al.* A Phase I clinical and pharmacological evaluation of sodium phenylbutyrate on a 120-h infusion schedule. *Clin Cancer Res* 2001; **7**: 3047–3055.

Oncogene (2005) 24, 157–164
© 2005 Nature Publishing Group All rights reserved 0950-9232/05 $30.00
www.nature.com/onc

Loss of heterozygosity and histone hypoacetylation of the *PINX1* gene are associated with reduced expression in gastric carcinoma

Tomohiro Kondo[1], Naohide Oue[1], Yoshitsugu Mitani[1], Hiroki Kuniyasu[2], Tsuyoshi Noguchi[3], Kazuya Kuraoka[1], Hirofumi Nakayama[1] and Wataru Yasui*[,1]

[1]*Department of Molecular Pathology, Hiroshima University Graduate School of Biomedical Sciences, 1-2-3 Kasumi, Minami-ku, Hiroshima 734-8551, Japan;* [2]*Department of Molecular Pathology, Nara Medical University, Kashihara, Japan;* [3]*Department of Oncological Science (Surgery II), Oita University Faculty of Medicine, Oita, Japan*

The expression of *PINX1*, a possible telomerase inhibitor and a putative tumor suppressor, has not been studied in human cancers, including gastric cancer (GC). We examined expression of *PINX1* by quantitative reverse transcription (RT)–PCR in 73 cases of GC, and 45 of these cases were further studied for loss of heterozygosity (LOH) by PCR with microsatellite marker D8S277. Reduced expression (tumor vs normal ratio <0.5) of *PINX1* was detected in 50 (68.5%) of 73 cases of GC. GC tissues with reduced expression of *PINX1* showed significantly higher telomerase activities as measured by telomeric repeat amplification protocol than those with normal expression of *PINX1* ($P=0.031$). LOH of *PINX1* locus was detected in 15 (33.3%) of 45 cases of GC and was correlated significantly with reduced expression of *PINX1* ($P=0.031$). Expression of *PINX1* in a GC cell line, MKN-74, was induced by treatment with trichostatin A (TSA) or nicotinamide (NAM). Chromatin immunoprecipitation assay of MKN-74 cells revealed that acetylation of histone H4 in the 5′ untranslated region (UTR) of *PINX1* was enhanced by treatment with TSA or NAM, whereas acetylation of histone H3 was not changed by TSA or NAM. In addition, TSA or NAM treatment led to inhibition of telomerase activity in MKN-74 cells. These results indicate that LOH of *PINX1* locus and hypoacetylation of histone H4 in the 5′ UTR of *PINX1* are associated with reduced expression of *PINX1* in GC. *Oncogene* (2005) **24**, 157–164. doi:10.1038/sj.onc.1207832

Keywords: *PINX1*; telomerase; LOH; histone H4; acetylation; hSir2; gastric carcinoma

Introduction

PinX1 is a Pin2/TRF1-binding protein that is a potent inhibitor of telomerase (Zhou and Lu, 2001). PinX1 binds human telomerase reverse transcriptase (hTERT) and inhibits its activity directly. A novel human liver-related putative tumor suppressor gene (*LPTS*) has been cloned previously (Liao *et al.*, 2000). *LPTS* gene is transcribed into two transcripts. The longer transcript, which is referred to as LPTS-L, encodes a 328-amino-acid protein (Liao *et al.*, 2002) that is highly homologous to PinX1 (Zhou and Lu, 2001). LPTS-L and PinX1 have different 3′-untranslated regions but encode the same protein, which is referred to as LPTS-L/PinX1 (Liao *et al.*, 2003). LPTS-L/PinX1 has strong telomerase inhibitory activity both *in vivo* and *in vitro* (Zhou and Lu, 2001; Liao *et al.*, 2002). A high percentage of tumor cells with characteristics of immortalization show high telomerase activity (Shay and Bacchetti, 1997; Cong *et al.*, 2002). We previously reported that telomerase activity is present in a majority of gastric cancer (GC) types (Tahara *et al.*, 1995; Yasui *et al.*, 1998, 1999). Loss of heterozygosity (LOH) of *LPTS-L/PINX1* locus, which maps to human chromosome 8p23, was identified in 34.5% of hepatocellular carcinoma cases (Park *et al.*, 2002). 8p23, but not specifically *PINX1*, is frequently deleted in various cancers, including carcinomas of the liver (Emi *et al.*, 1992), lung (Ohata *et al.*, 1993), colorectum (Fujiwara *et al.*, 1993), prostate (Macoska *et al.*, 1995), and breast (Yaremko *et al.*, 1995), in addition to GC (Yustein *et al.*, 1999; Baffa *et al.*, 2000). However, the significance of the *LPTS-L/PINX1* gene in human cancers including GC remains unclear.

A variety of genetic and epigenetic alterations are associated with GC (Yasui *et al.*, 2000; Oue *et al.*, 2004). Several lines of evidence suggest that histone acetylation plays an important role in transcriptional regulation (Grunstein, 1997). Histone hyperacetylation is thought to relax the chromatin structure and allow transcription factors to access promoters (Luger *et al.*, 1997; Luger and Richmond, 1998). We have reported that trichostatin A (TSA), a histone deacetylase (HDAC) inhibitor, induces expression of $p21^{Waf1}$ and *HLTF* in GC cell lines (Suzuki *et al.*, 2000; Hamai *et al.*, 2003). HDACs are separated into three distinct classes on the basis of their homologies to yeast transcriptional repressors (North *et al.*, 2003). Class I and II deacetylases are homologs of the yeast Rpd3p and Hda1p proteins, respectively. Class III deacetylases are classified on the basis of homology to the yeast transcriptional repressor, Sir2, which is nicotinamide adenine dinucleotide (NAD)-dependent HDAC (Imai *et al.*, 2000; Landry *et al.*, 2000; Smith

*Correspondence: W Yasui; E-mail: wyasui@hiroshima-u.ac.jp
Received 3 December 2003; revised 22 April 2004; accepted 22 April 2004

et al., 2000). TSA inhibits class I and II deacetylases, whereas nicotinamide (NAM) inhibits hSir2 (Luo *et al.*, 2001; Bitterman *et al.*, 2002).

In the present study, we examined expression and LOH of *PINX1* locus in GC. We also examined the association between expression of *PINX1* and acetylation of histones in the 5′ untranslated region (UTR) of *PINX1* in GC cell lines.

Results

Expression of PINX1 *in GC*

Levels of *PINX1* expression in 73 cases of GC are shown in Figure 1a. *PINX1* levels were significantly lower in GC tissues (0.347 ± 0.138) than in non-neoplastic mucosa (1.766 ± 0.758, $P < 0.0001$, Wilcoxon signed rank test). Reduced expression of *PINX1* (tumor *vs* normal ratio < 0.5) was detected in 50 (68.5%) of 73 cases of GC. Reduced expression of *PINX1* in GC tissues was not significantly associated with T grade (depth of tumor invasion), N grade (degree of lymph node metastasis), tumor stage, or histological type (Table 1).

Correlation between expression of PINX1 and telomerase activity in GC

We examined the correlation between *PINX1* expression and telomerase activity in 20 of 73 cases of GC. GC tissues with reduced expression of *PINX1* showed significantly higher telomerase activities than those with normal expression of *PINX1* (4.608 ± 2.596 *vs* 1.438 ± 1.018, $P = 0.031$, Mann–Whitney *U*-test, Figure 1b).

LOH analysis of PINX1 locus in GC

LOH analysis was performed for 45 of 73 cases of GC, and representative results are shown in Figure 2a. LOH of *PINX1* locus was detected in 15 (33.3%) of 45 cases of GC. Of 15 cases with LOH of *PINX1* locus, 14 (93.3%) showed reduced expression of *PINX1* (Figure 2b and Table 2). Reduced expression of *PINX1* was significantly associated with LOH of *PINX1* locus ($P = 0.031$; Fisher's exact test). LOH of *PINX1* locus was not significantly associated with T grade, N grade, tumor stage, or histological type.

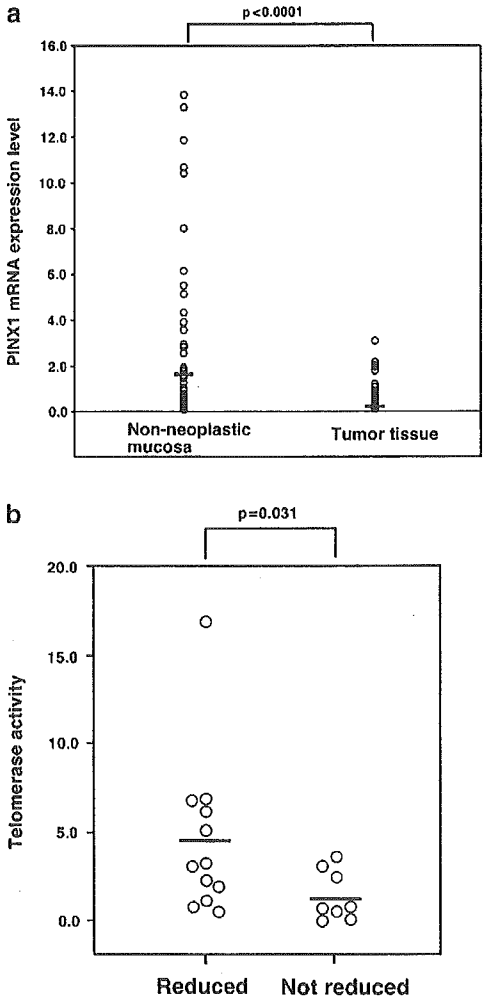

Figure 1 Expression of *PINX1* in GC. (**a**) Quantitative RT–PCR analysis of GC tissues and corresponding non-neoplastic mucosae. Expression of *PINX1* was significantly lower in GC tissues than in corresponding non-neoplastic mucosae ($P < 0.0001$, Wilcoxon signed rank test). The expression value was calculated as the mean of three independent quantitative RT–PCR experiments. The units are arbitrary, and we calculated the *PINX1* mRNA expression level by standardization against 1 μg of total RNA from HSC-39 GC cells, which was taken as 1.0. (**b**) Correlation between telomerase activity and reduced expression of *PINX1*. Reduced ($T/N < 0.5$), not reduced ($T/N \geq 0.5$). Telomerase activities were higher in GC tissues with reduced expression of *PINX1* than in those with normal *PINX1* levels ($P = 0.031$, Mann–Whitney *U*-test). We examined the correlation between *PINX1* expression levels and telomerase activity in 20 of 73 cases for which telomerase activities were reported (Yasui *et al.*, 1998)

PINX1 expression status in GC cell lines

Next, we performed experiments with eight GC cell lines to further analyse *PINX1* expression status. Quantitative RT–PCR analysis revealed that the average level of *PINX1* expression in eight GC cell lines (0.691 ± 0.226) was less than a half of that in non-neoplastic mucosa of 73 cases (1.766 ± 0.758) (Figure 3a). In particular, *PINX1* expression level in MKN-74 cells was obviously lower than that in the seven other GC cell lines. Methylation of CpG island is an alternative way of causing the gene silencing of diverse tumor suppressor genes. To evaluate the extent of the *PINX1* methylation, bisulfite sequencing was carried out in three cell lines (MKN-28, MKN-74, and HSC-39). The *PINX1* CpG islands of these cell lines were found to be little methylated over the entire region analysed (Figure 3b and Table 3). To further examine if the reduced expression of *PINX1* is related to genomic alteration of the gene, Southern blot was performed in eight GC cell lines. No obvious alteration of *PINX1* was found in all cell lines (Figure 3c).

Table 1 Clinicopathological features of gastric cancers ($n=73$) and reduced expression of *PINX1*

	Reduced (T/N[a] *<0.5)*	*Not reduced* (T/N *≥0.5)*	P-*value*[b]
Histology[c]			
Intestinal	24 (63.2%)	14	
Diffuse	26 (74.3%)	9	0.221
T grade[d]			
T1, 2	22 (62.9%)	13	
T3, 4	28 (73.7%)	10	0.229
N grade[d]			
N0	14 (70.0%)	6	
N1, 2, 3	36 (67.9%)	17	0.551
Stage[d]			
I, II	20 (69.0%)	9	
III, IV	30 (68.2%)	14	0.576

[a]*T/N* ratio, *PINX1* mRNA expression levels in GC tissue relative to levels in corresponding non-neoplastic mucosa. [b]Fisher's exact test. [c]According to the Lauren criteria (Lauren, 1965). [d]According to the criteria of the TNM Stage classification system (Sobin and Wittekind, 1997)

PINX1 expression was induced by treatment with TSA and NAM

Histone acetylation plays an important role in gene expression. We presumed the possibility that histone acetylation is involved in reduced *PINX1* expression. Treatment of MKN-74 cells with TSA, an HDAC (class I and II) inhibitor, and NAM, an hSir2 (class III) inhibitor, increased *PINX1* expression in the cells (Figure 4a). The treatment with TSA and NAM together yielded an additive increase in *PINX1* expression in MKN-74 cells. In contrast, in MKN-28 cells, treatment with TSA and NAM had no effect on *PINX1* expression.

Histone acetylation status of the PINX1 gene in GC cell lines

To examine acetylation of histones H3 and H4 in the 5′ UTR of *PINX1* in MKN-74 cells, we performed chromatin immunoprecipitation (ChIP) assays. The level of acetylation of histone H3 in the 5′ UTR of *PINX1* in MKN-74 cells was similar to that in MKN-28 cells (Figure 4b). Moreover, no change in the level of acetylation of histone H3 in the 5′ UTR of *PINX1* was observed in MKN-74 cells treated with TSA and NAM. However, acetylation of histone H4 in the 5′ UTR of *PINX1* in MKN-74 cells was significantly lower than that in MKN-28 cells (Figure 4c). After treatment with both TSA and NAM, acetylation of histone H4 in the 5′ UTR of *PINX1* was increased in MKN-74 cells. No significant changes in histone H4 acetylation were observed in MKN-28 cells (data not shown).

Alteration of telomerase activity in MKN-74 treated with TSA and NAM

PinX1 binds to hTERT and inhibits its activity directly (Zhou and Lu, 2001). To observe the alteration of telomerase activity when *PINX1* expression is changed, we performed telomeric repeat amplification protocol (TRAP) assay in MKN-74 cells treated with TSA and NAM. Telomerase activity was reduced to 65.6% with TSA, and to 10.2% with NAM (Figure 5a). Levels of *hTERT* expression were not significantly changed by treatment with TSA or NAM (Figure 5b).

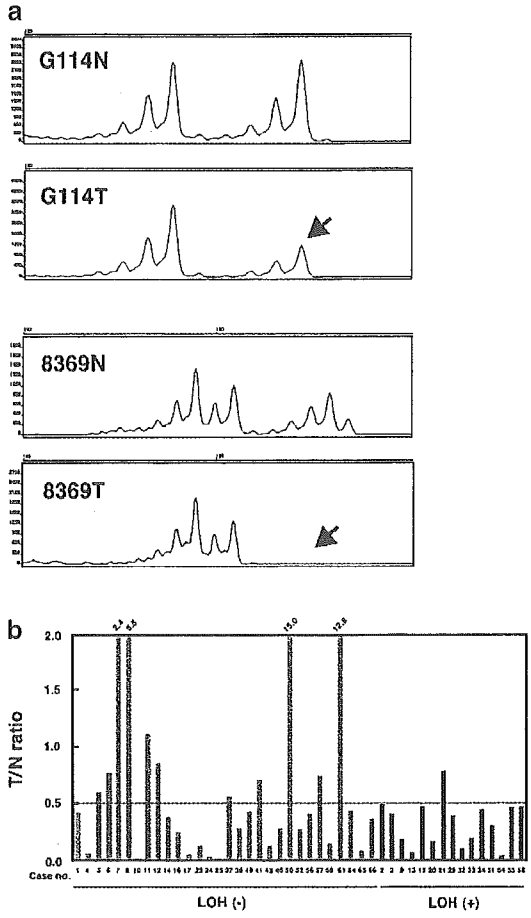

Figure 2 LOH of *PINX1* locus in GC specimens and association between LOH and *PINX1* expression. (**a**) Representative fluorescent electropherograms for LOH. Tumor tissues (T), corresponding non-neoplastic mucosae (N). Lost alleles are indicated by arrows. (**b**) Distribution of *PINX1* expression in 45 cases of GC. *T/N* ratio, *PINX1* mRNA expression levels in GC tissue relative to levels in corresponding non-neoplastic mucosa. *T/N*<0.5-fold is defined as reduced expression of *PINX1*

Discussion

The *PINX1* gene appears to function as a tumor suppressor; however, the association between *PINX1* and GC has not been studied. We report here reduced expression of *PINX1* in 50 (68.5%) of 73 GC cases. In all, 15 (33.3%) of 45 cases had LOH of *PINX1* locus, which was correlated significantly with reduced expression of *PINX1*, suggesting that LOH plays a major role in reduced expression of *PINX1*. We did not find any association between reduced expression of *PINX1* and

Table 2 Clinicopathological features of gastric cancers ($n=45$) and LOH of *PINX1* locus

	LOH		P-*value*[a]
	(+)	*(−)*	
PINX1 expression			
Reduced ($T/N<0.5$)	14 (42.4%)	19	
Not reduced ($T/N\geqslant 0.5$)	1 (8.3%)	11	0.031
Histology			
Intestinal	7 (33.3%)	14	
Diffuse	8 (33.3%)	16	0.625
T grade			
T1,2	8 (34.8%)	15	
T3,4	7 (31.8%)	15	0.542
N grade			
N0	4 (33.3%)	8	
N1,2,3	11 (33.3%)	22	0.645
Stage			
I,II	5 (27.8%)	13	
III,IV	10 (37.0%)	17	0.376

[a]Fisher's exact test

frequency of LOH and T grade, N grade, or tumor stage. This finding suggests that downregulation of *PINX1* may be involved in tumor development but not in tumor progression. We also found that telomerase activity is higher in GC tissues with reduced expression of *PINX1* than in those with normal levels of *PINX1*. Reduced expression of *PINX1* appears to be involved in activation of telomerase. Since *PINX1* is located in the subtelomeric region of human chromosome 8, LOH of the *PINX1* locus may occur easily through telomere dysfunction and chromosome instability during initiation of human cancers (Chin *et al*., 1999; Artandi *et al*., 2000; DePinho, 2000; O'Sullivan *et al*., 2002; Meeker *et al*., 2002; Van Heek *et al*., 2002). Recently, we reported that inhibition of Pot1, a single-stranded telomeric DNA-binding protein, induces telomere dysfunction and that expression of *POT1* is reduced in early-stage GC (Kondo *et al*., 2004). Although hTERT, the catalytic subunit of telomerase, is essential for activation of telomerase, it is possible that downregulation of *PINX1*, due to LOH, contributes to activation of telomerase at an early stage of stomach carcinogenesis. In fact, we previously observed that telomerase is activated in precancerous conditions such as intestinal metaplasia and adenoma of the stomach (Tahara *et al*., 1995; Kuniyasu *et al*., 1997; Yasui *et al*., 1999). Activation of telomerase is essential for cell immortality, and it may be a critical step in the development of cancers (Tahara *et al*., 1995). PinX1 may inhibit telomerase activation in normal somatic cells.

We observed reduced expression of *PINX1* in 19 (63.3%) of 30 cases of GC that did not have LOH of *PINX1* locus. We hypothesized that DNA methylation

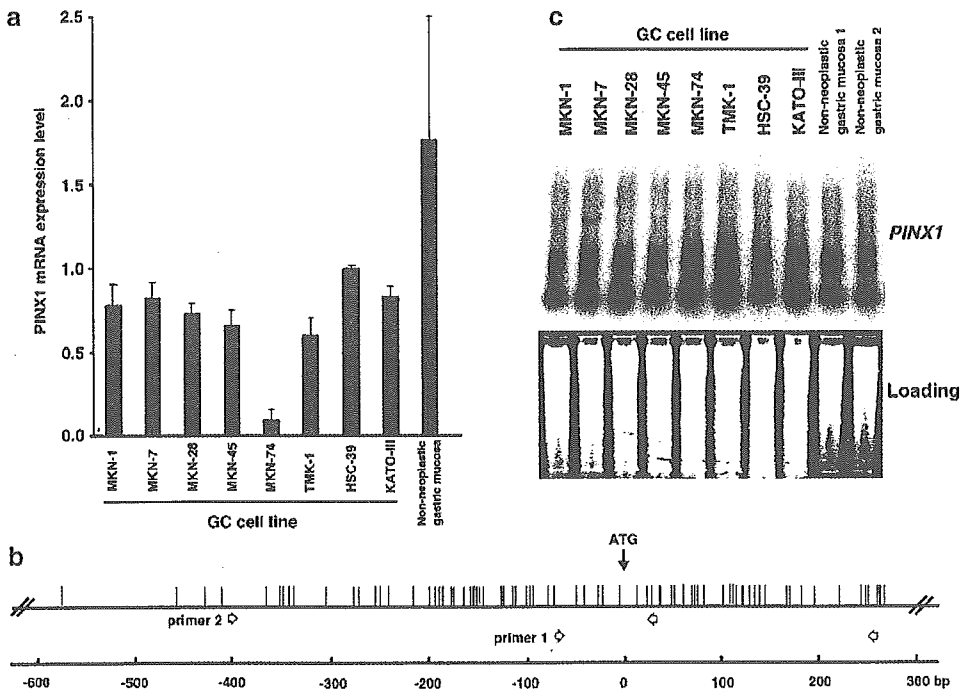

Figure 3 Expression of *PINX1* in GC cell lines. (**a**) Quantitative RT–PCR analysis of GC cell lines. Expression of *PINX1* in MKN-74 cells was lower than that in seven other GC cell lines. Each value is the mean of three independent quantitative RT–PCR experiments. Error bars indicate standard error (s.e.) from the mean. The units are arbitrary, and we calculated the level of *PINX1* expression by standardization against 1 μg of total RNA from HSC-39 GC cells, which was taken as 1.0. (**b**) A map of the CpG island of the *PINX1* gene. The CpG map of the sequence around exon 1 of the *PINX1* gene is shown. The CpG density is indicated by short vertical bars. Arrows represent PCR primers. The numbering in this scheme corresponds to position relative to known translation start sites. (**c**) Southern blot analysis of the *PINX1* gene in eight GC cell lines. All cell lines showed no change of *PINX1* status in comparison with normal gastric mucosa

Table 3 DNA methylation status of 38 CpG islands in the *PINX1*

Sample	*Expression*[a]	*CpG islands, percentage of clones exhibiting methylation*[b]																																					
		1	*2*	*3*	*4*	*5*	*6*	*7*	*8*	*9*	*10*	*11*	*12*	*13*	*14*	*15*	*16*	*17*	*18*	*19*	*20*	*21*	*22*	*23*	*24*	*25*	*26*	*27*	*28*	*29*	*30*	*31*	*32*	*33*	*34*	*35*	*36*	*37*	*38*
MKN-28	M	0	0	0	0	0	0	0	0	0	0	0	0	0	0	0	0	0	0	0	0	0	0	0	0	0	0	0	0	0	0	10	10	0	0	0	0	0	0
MKN-74	L	0	0	0	0	0	0	0	0	0	0	0	0	0	0	0	0	0	0	0	0	0	0	0	10	0	0	0	0	0	0	0	0	0	0	0	0	0	0
HSC-39	M	20	30	20	0	0	0	0	0	0	0	0	0	0	0	0	0	0	0	0	0	0	0	0	0	0	10	0	0	0	0	0	0	0	0	0	0	0	0

[a]*PINX1* expression determined with quantitative RT–PCR. We calculated the level of *PINX1* expression by standardization against 1 μg of total RNA from HSC-39 cells, which was taken as 1.0. Units of expression levels were divided into three groups: Low, 0–0.5 U calculated (L); Medium, 0.5–2.0 U calculated (M); High, >2.0 U calculated (H). [b]DNA extracted from each sample was treated with sodium bisulfite and described in 'Materials and methods'. The percentage of 10 independent clones exhibiting DNA methylation at each CpG island is listed

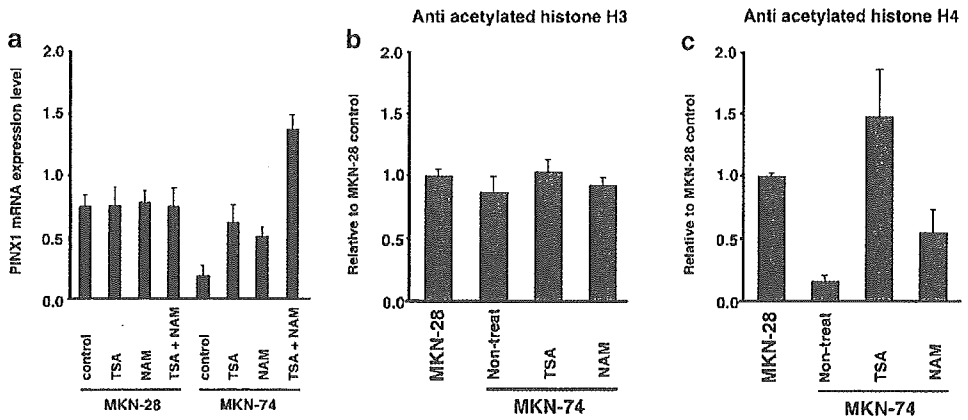

Figure 4 Effect on *PINX1* expression of TSA and NAM in GC cell lines. (**a**) Quantitative RT–PCR analysis of TSA- and/or NAM-treated MKN-28 and MKN-74 cells. We treated GC cell lines with TSA for 24 h and with NAM for 6 h. Cotreatment with TSA and NAM was performed for 12 h. In MKN-74 cells, treatment with TSA and/or NAM increased *PINX1* expression, whereas in MKN-28 cells, treatment with TSA and/or NAM did not significantly alter *PINX1* expression. (**b**, **c**) ChIP assay of MKN-28 and MKN-74 cells. Levels of acetylation of histone H3 in the 5′ UTR of *PINX1* in MKN-74 cells were similar to those in MKN-28 cells. Acetylation levels did not change in response to treatment with TSA or NAM. Levels of acetylation of histone H4 in the 5′ UTR of *PINX1* in MKN-74 cells were significantly lower than those in MKN-28 cells. After treatment with both TSA and NAM, acetylation of histone H4 in the 5′ UTR of *PINX1* was increased in MKN-74 cells. Bar graphs illustrate the levels of acetylation of histones H3 and H4 in MKN-74 cells relative to those of histones H3 and H4 in MKN-28 cells. Each value is the mean of three independent ChIP experiments. Error bars indicate SE from the mean. The units are arbitrary, and we calculated the acetylation level by standardization with the value from 0.1 μg of genomic DNA of HSC-39 GC cells, which was taken as 1.0

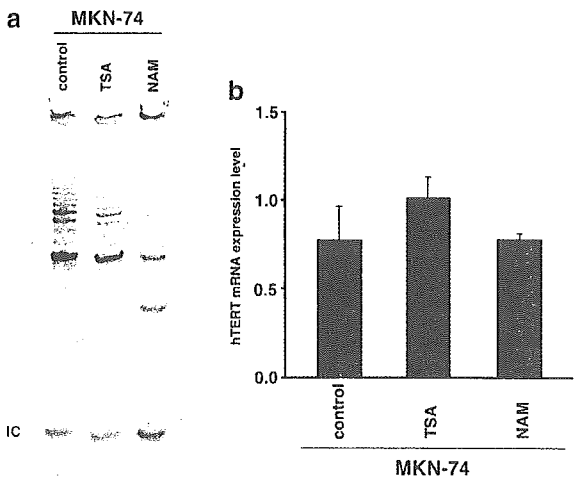

Figure 5 Alteration of telomerase activity and *hTERT* expression in MKN-74 treated with TSA and NAM. (**a**) Reduced telomerase activity was detected in TSA- and NAM-treated MKN-74 cells. IC = internal control (36 bp). (**b**) *hTERT* expression did not significantly change in TSA- and NAM-treated MKN-74 cells

might contribute to reduced expression of *PINX1* in such cases because hypermethylation of CpG islands in promoters is associated with silencing of many tumor suppressor genes in human cancers (Razin and Cedar, 1991; Kass *et al*., 1997; Jones and Baylin, 2002). We have also reported DNA methylation of tumor suppressor genes in GC (Oue *et al*., 2001, 2002, 2003; Hamai *et al*., 2003; Oshimo *et al*., 2004). Although the average level of *PINX1* expression in eight GC cell lines (0.691 ± 0.226) showed less than half that in non-neoplastic mucosa of 73 GC cases (1.766 ± 0.758), complete silencing of *PINX1* expression was not observed and bisulfite sequencing revealed that the *PINX1* CpG island methylation were little over the entire region analysed in MKN-28, MKN-74, and HSC-39 cells. Recently, it has been reported that the *PINX1* promoter is not hypermethylated in GC tissues (Akiyama *et al*., 2004).

We then investigated the possibility that histone acetylation status alters expression of *PINX1*. Both TSA and NAM treatment induce *PINX1* expression in MKN-74 cells, and acetylation of histone H4 in the 5′

UTR of *PINX1* is increased, whereas acetylation of histone H3 is not changed significantly. These data suggest that hypoacetylation of histone H4 in the 5′ UTR of *PINX1* reduces expression of *PINX1*.

Our results also indicated that *PINX1* acetylation may be controlled through two pathways of histone deacetylation. The first pathway may involve class I and/or II HDACs. The second pathway is inhibited by NAM, which suggests the involvement of the NAD-dependent TSA-resistant Sir2 deacetylase, which is a class III HDAC. Deacetylation by Sir2 occurs selectively at Lys 16 of histone H4 in yeast (Imai *et al.*, 2000). Therefore, we believe that acetylation of histone H4 in the 5′ UTR of *PINX1* was induced selectively by NAM in the present study.

Moreover, we revealed that telomerase activity was inhibited with TSA and NAM in MKN-74 cells, although *hTERT* expression was not changed. Thus, PinX1 inhibits telomerase activity without change of *hTERT* expression. Our results also provide a possibility for cancer therapy with NAM.

In conclusion, our data show that LOH of the *PINX1* locus and hypoacetylation of histone H4 in the 5′ UTR of *PINX1* are associated with reduced expression of *PINX1* in GC. However, we cannot exclude the possibility that reduced expression of *PINX1* is associated with mutation or other factors. Further studies may provide a better understanding of the physiological function of *PINX1* and its role as a tumor suppressor in stomach carcinogenesis.

Materials and methods

Tissue samples

A total of 73 GC samples from 73 patients were studied. Tumors and corresponding non-neoplastic mucosae were removed surgically at Hiroshima University Hospital, frozen immediately in liquid nitrogen, and stored at −80°C until use. We confirmed microscopically that the carcinoma tissue specimens consisted mainly (>80%) of carcinoma tissue, and that the non-neoplastic mucosae did not show any invasion by carcinoma cells or show significant inflammatory involvement. Histologic classification and tumor staging were carried out according to the Lauren classification system (Lauren, 1965) and the TNM Stage Grouping (UICC 5th Edition, 1997) (Sobin and Wittekind, 1997). Telomerase activities were determined previously in 20 of the 73 GC samples by TRAP analysis (Yasui *et al.*, 1998).

Cell lines and drug treatment

Eight cell lines derived from human GC were used. The TMK-1 cell line was established in our laboratory from a poorly differentiated adenocarcinoma (Ochiai *et al.*, 1985). Five GC cell lines of the MKN series (MKN-1, adenosquamous cell carcinoma; MKN-7, MKN-28, and MKN-74, well-differentiated adenocarcinomas; and MKN-45, poorly differentiated adenocarcinoma) were kindly provided by Dr T Suzuki. KATO-III and HSC-39 cell lines, which were established from signet ring cell carcinomas, were kindly provided by Dr M Sekiguchi and Dr K Yanagihara (Yanagihara *et al.*, 1991), respectively. All cell lines were routinely maintained in RPMI 1640 (Nissui Pharmaceutical Co., Ltd, Tokyo, Japan) containing 10% fetal bovine serum (FBS) (Bio-Whittaker, Walkersville, MD, USA) in a humidified atmosphere of 5% CO_2 and 95% air at 37°C. MKN-28 and MKN-74 cells were treated with 300 nM TSA (Wako, Tokyo, Japan) for 24 h or with 5 mM NAM (Sigma, St Louis, MO, USA) for 6 h.

Quantitative RT–PCR

Total RNA was extracted from tissues and cell lines with the RNeasy Mini Kit (Qiagen, Valencia, CA, USA). Total RNA (1 μg) was converted to cDNA with the First-Strand cDNA Synthesis Kit (Amersham Pharmacia Biotech, Uppsala, Sweden). To analyse the expression of *PINX1* gene in GC tissues specimens and GC cell lines, we performed real-time RT–PCR. PCRs were performed with the SYBR Green PCR Core Reagent kit (Applied Biosystems, Foster City, CA, USA). Real-time detection of the emission intensity of SYBR Green bound to double-stranded DNAs was performed with the ABI PRISM 7700 Sequence Detection System (Applied Biosystems). The *PINX1* cDNA and the *ACTB* cDNA (internal control) were amplified separately. Relative gene expression was determined from the threshold cycle for the *PINX1* gene and the *ACTB* gene. Reference samples (HSC-39) were included on each assay plate to verify plate-to-plate consistency. Plates were normalized to each other with these reference samples. PCR amplification was performed in 96-well optical trays with caps with a 25 μl final reaction mixture according to the manufacturer's instructions. Quantitative RT–PCRs were performed in triplicate for each sample and primer set, and the mean of the three experiments was used as the relative quantification value. We analysed *PINX1* levels in 73 cases of GC by calculating the ratio of *PINX1* mRNA expression levels between carcinoma tissue and the corresponding non-neoplastic mucosa (*T*/*N* ratio). We considered a $T/N<0.5$-fold to indicate reduced expression of *PINX1*. *PINX1* primer sequences were 5′-CAC TCC AGA GGA GAA CGA AAC C-3′ (sense) and 5′-CAC CGG CTT GGC AAA GTA CT-3′ (antisense). *ACTB* primer sequences were 5′-TCA CCG AGC GCG GCT-3′ (sense) and 5′-TAA TGT CAC GCA CGA TTT CCC-3′ (antisense). We used TaqMan Pre-Developed Assay Reagents Human TERT and TaqMan β-actin Control Reagents (Applied Biosystems) in *hTERT* expression analysis.

Genomic DNA extraction and LOH analysis

To examine LOH of *PINX1* locus, we extracted genomic DNAs from GC tissues with a genomic DNA purification kit (Promega, Madison, WI, USA). LOH at microsatellite marker D8S277 was evaluated by PCR of tumor and normal specimens, and microcapillary electrophoresis of PCR products was carried out in an ABI PRISM 310 Genetic Analyzer (Applied Biosystems). GeneScan software (Applied Biosystems) was used to quantify and interpret the raw data. Allelic loss was calculated according to a previously described formula (Liloglou *et al.*, 2000, 2001). Among 73 GC cases, we evaluated 45 cases for which genomic DNA was available.

Bisulfite genomic DNA sequencing

To examine the DNA methylation patterns, we treated genomic DNA with sodium bisulfite, as described previously (Hermann *et al.*, 1996). In brief, 2 μg of genomic DNA was denatured by treatment with NaOH and modified with 3 M sodium bisulfite for 16 h. DNA samples were purified with Wizard DNA purification resin (Promega), treated with NaOH, precipitated with ethanol, and resuspended in 25 μl

of water. Treated DNAs were stored at −20°C until needed. Sodium bisulfite-treated genomic DNAs were amplified with *PINX1* gene-specific primers (primer 1 and primer 2, Figure 3b). Primer 1 sequences were 5′-TTT GAT TTT TTT GGA GTT TTT AGT-3′ (sense) and 5′-GCG ACC CAA AAT AAT TCT AAA-3′ (antisense). Primer 2 sequences were 5′-GGG TTT TTT GAT GGA GAT TTT A-3′ (sense) and 5′-ACG TTC AAC CAA CAT AAA CAT ATC-3′ (antisense). Conditions for the PCR were 1 cycle at 94°C for 10 min; 34 cycles at 94°C for 1 min, at 54°C for 1 min, and at 72°C for 1 min, and 1 cycle at 72°C for 4 min. The PCR product was cloned into the TA vector pCR2.1 (Invitrogen, Carlsbad, CA, USA). A total of 10 subclones were confirmed by restriction analysis and sequenced using the M13 reverse primer (Invitrogen) with a Prism 310 DNA Sequencer (Perkin-Elmer Applied Biosystems).

ChIP assay

ChIP assay of GC cell lines was performed as described previously with modification (Ferreira *et al*., 2001). In brief, chromatin proteins were crosslinked to DNA by addition of formaldehyde directly to the culture medium to a final concentration of 1%. After 10-min incubation at room temperature, the cells were washed and scraped off the dishes into ice-cold phosphate-buffered saline (PBS) containing protease inhibitors. Cells were pelleted and then resuspended in SDS lysis buffer (1% SDS, 10 mM EDTA, 50 mM Tris-HCl, pH 8.1, protease inhibitor) for 10 min on ice. The lysate was sonicated to reduce the mean DNA fragment size to 300–1000 bp. The sample was centrifuged to remove cell debris and diluted 10-fold in ChIP dilution buffer (0.01% SDS, 1.1% Triton X-100, 1.2 mM EDTA, 16.7 mM Tris-HCl, pH 8.1, 167 mM NaCl, protease inhibitors). The chromatin solution was precleared with 40 μl of a mixture of salmon sperm DNA–protein A agarose slurry (Upstate Biotechnology, Lake Placid, NY, USA) to reduce nonspecific background. After precleaning, the solution was centrifuged, and the supernatant was collected. In all, 5 μl of either antiacetylated histone H3 or H4 antibody (Upstate Biotechnology) was added to the chromatin solution and incubated overnight at 4°C with agitation. A no-antibody control was also performed for each ChIP assay. After the overnight incubation, immune complexes were collected by addition of 60 μl of salmon sperm DNA–protein A agarose slurry (Upstate Biotech) and incubated at 4°C with agitation for 1 h. Beads were washed five times, and the bound immune complexes were eluted with buffer containing 1% SDS and 0.1 M $NaHCO_3$. Crosslinks were reversed by addition of 5 M NaCl and incubation at 65°C for 4 h. Samples were then treated with proteinase K for 1 h, and DNA was purified by phenol/chloroform extraction and ethanol precipitation. We performed PCR analysis of immunoprecipitated DNA using primers specific for the 5′ region of the *ACTB* gene. Each PCR product (15 μl) was loaded onto 8% nondenaturing polyacrylamide gels, separated by electrophoresis, stained with ethidium bromide, and visualized under UV light to confirm that there was no genomic DNA contamination of the no-antibody control. For quantitative PCR analysis of immunoprecipitated DNAs, we performed real-time PCR as described above.

PINX1 primer (5′ region) sequences were 5′-CCT GAG TCC AGT GCC CTA CTT T-3′ (sense) and 5′-GAA TTT TCC CAG CCA AGG C-3′ (antisense). *ACTB* primer (5′ region) sequences were 5′-CCC ACC CGG TCT TGT GTG-3′ (sense) and 5′-GGG AAG ACC CTG TCC TTG TCA-3′ (antisense).

Southern blot analysis

High molecular weight genomic DNA was extracted with a DNA Extraction Kit (Stratagene Cloning System, La Jolla, CA, USA). Tissue DNA was digested with *Msp*I, electrophoresed on 0.6% agarose gels, and blotted onto nitrocellulose filters. The filters were hybridized with the full-length cDNA PINX1 probe and then autoradiographed.

TRAP assay

TRAP assay was carried out with a TRAPEZE Telomerase Detection Kit (Intergen Company, Oxford, UK). Intensity of the TRAP product bands and of the internal control bands was determined with the use of NIH Image.

Statistical analysis

Statistical significance was assessed by Wilcoxon signed rank test, Mann–Whitney *U*-test, or Fisher's exact test. StatView 5.0 Macintosh software was used. The *P*-values of less than 0.05 were considered statistically significant.

Acknowledgements
We thank Mr M Takatani and Ms M Ueda for their excellent technical assistance and advice.

References

Akiyama Y, Maesawa C, Wada K, Fujisawa K, Itabashi T, Noda Y, Honda T, Sato N, Ishida K, Takagane A, Saito K and Masuda T. (2004). *Oncol. Rep.*, **11,** 871–874.
Artandi SE, Chang S, Lee SL, Alson S, Gottlieb GJ, Chin L and DePinho RA. (2000). *Nature*, **406,** 641–645.
Baffa R, Santoro R, Bullrich F, Mandes B, Ishii H and Croce CM. (2000). *Clin. Cancer Res.*, **6,** 1372–1377.
Bitterman KJ, Anderson RM, Cohen HY, Latorre-Esteves M and Sinclair DA. (2002). *J. Biol. Chem.*, **277,** 45099–45107.
Chin L, Artandi SE, Shen Q, Tam A, Lee SL, Gottlieb GJ, Greider CW and DePinho RA. (1999). *Cell*, **97,** 527–538.
Cong YS, Wright WE and Shay JW. (2002). *Microbiol. Mol. Biol. Rev.*, **66,** 407–425.
DePinho RA. (2000). *Nature*, **408,** 248–254.
Emi M, Fujiwara Y, Nakajima T, Tsuchiya E, Tsuda H, Hirohashi S, Maeda Y, Tsuruta K, Miyaki M and Nakamura Y. (1992). *Cancer Res.*, **52,** 5368–5372.
Ferreira R, Naguibneva I, Mathieu M, Ait-Si-Ali S, Robin P, Pritchard LL and Harel-Bellan A. (2001). *EMBO Rep.*, **2,** 794–799.
Fujiwara Y, Emi M, Ohata H, Kato Y, Nakajima T, Mori T and Nakamura Y. (1993). *Cancer Res.*, **53,** 1172–1174.
Grunstein M. (1997). *Nature*, **389,** 349–352.
Hamai Y, Oue N, Mitani Y, Nakayama H, Ito R, Matsusaki K, Yoshida K, Toge T and Yasui W. (2003). *Cancer Sci.*, **94,** 692–698.
Herman JG, Graff JR, Myohanen S, Nelkin BD and Baylin SB. (1996). *Proc. Natl. Acad. Sci. USA*, **93,** 9821–9826.
Imai S, Armstrong CM, Kaeberlein M and Guarente L. (2000). *Nature*, **403,** 795–800.
Jones PA and Baylin SB. (2002). *Nat. Rev. Genet.*, **3,** 415–428.
Kass SU, Pruss D and Wolffe AP. (1997). *Trends Genet.*, **13,** 444–449.

Kondo T, Oue N, Yoshida K, Mitani Y, Naka K, Nakayama H and Yasui W. (2004). *Cancer Res.*, **64,** 523–529.
Kuniyasu H, Domen T, Hamamoto T, Yokozaki H, Yasui W, Tahara H and Tahara E. (1997). *Jpn. J. Cancer Res.*, **88,** 103–107.
Landry J, Sutton A, Tafrov ST, Heller RC, Stebbins J, Pillus L and Sternglanz R. (2000). *Proc. Natl. Acad. Sci. USA*, **97,** 5807–5811.
Lauren P. (1965). *Acta. Pathol. Microbiol. Scand.*, **64,** 31–49.
Liao C, Zhao M, Song H, Uchida K, Yokoyama KK and Li T. (2000). *Hepatology*, **32,** 721–727.
Liao C, Zhao MJ, Zhao J, Jia D, Song H and Li ZP. (2002). *World J. Gastroentrol.*, **8,** 1050–1052.
Liao C, Zhao MJ, Zhao J, Song H, Pineau P, Marchio A, Dejean A, Tiollais P, Wang HY and Li TP. (2003). *World J. Gastroentrol.*, **9,** 89–93.
Liloglou T, Maloney P, Xinarianos G, Fear S and Field JK. (2000). *Int. J. Oncol.*, **16,** 5–14.
Liloglou T, Maloney P, Xinarianos G, Hulbert M, Walshaw MJ, Gosney JR, Turnbull L and Field JK. (2001). *Cancer Res.*, **61,** 1624–1628.
Luger K, Mader AW, Richmond RK, Sargent DF and Richmond TJ. (1997). *Nature*, **389,** 251–260.
Luger K and Richmond TJ. (1998). *Curr. Opin. Genet. Dev.*, **8,** 140–146.
Luo J, Nikolaev AY, Imai S, Chen D, Su F, Shiloh A, Guarente L and Gu W. (2001). *Cell*, **107,** 137–148.
Macoska JA, Trybus TM, Benson PD, Sakr WA, Grignon DJ, Wojno KD, Pietruk T and Powell IJ. (1995). *Cancer Res.*, **55,** 5390–5395.
Meeker AK, Hicks JL, Platz EA, March GE, Bennett CJ, Delannoy MJ and De Marzo AM. (2002). *Cancer Res.*, **62,** 6405–6409.
North BJ, Marshall BL, Borra MT, Denu JM and Verdin E. (2003). *Mol. Cell*, **11,** 437–444.
Ochiai A, Yasui W and Tahara E. (1985). *Jpn. J. Cancer Res.*, **76,** 1064–1071.
Ohata H, Emi M, Fujiwara Y, Higashino K, Nakagawa K, Futagami R, Tsuchiya E and Nakamura Y. (1993). *Genes Chromosomes Cancer*, **7,** 85–88.
Oshimo Y, Oue N, Mitani Y, Nakayama H, Kitadai Y, Yoshida K, Chayama K and Yasui W. (2004). *Int. J. Cancer*, **110,** 212–218.
O'Sullivan JN, Bronner MP, Brentnall TA, Finley JC, Shen WT, Emerson S, Emond MJ, Gollahon KA, Moskovitz AH, Crispin DA, Potter JD and Rabinovitch PS. (2002). *Nat. Genet.*, **32,** 280–284.
Oue N, Hamai Y, Mitani Y, Matsumura S, Oshimo Y, Aung PP, Kuraoka K, Nakayama H and Yasui W. (2004). *Cancer Res.*, **64,** 2397–2405.
Oue N, Matsumura S, Nakayama H, Kitadai Y, Taniyama K, Matsusaki K and Yasui W. (2003). *Oncology*, **64,** 423–429.
Oue N, Motoshita J, Yokosaki H, Hayashi K, Tahara E, Taniyama K, Matsusaki K and Yasui W. (2002). *J. Pathol.*, **198,** 55–59.
Oue N, Shigeishi H, Kuniyasu H, Yokosaki H, Kuraoka K, Ito R and Yasui W. (2001). *Int. J. Cancer*, **93,** 805–809.
Park WS, Lee JH, Park JY, Jeong SW, Shin MS, Kim HS, Lee SK, Lee SN, Lee SH, Park CG, Yoo NJ and Lee JY. (2002). *Cancer Lett.*, **178,** 199–207.
Razin A and Cedar H. (1991). *Microbil. Rev.*, **55,** 451–458.
Shay JW and Bacchetti S. (1997). *Eur. J. Cancer*, **33,** 787–791.
Smith JS, Brachmann CB, Celic I, Kenna MA, Muhammad S, Starai VJ, Avalos JL, Escalante-Semerena JC, Grubmeyer C, Wolberger C and Boeke JD. (2000). *Proc. Natl. Acad. Sci. USA*, **97,** 6658–6663.
Sobin LH and Wittekind CH (ed). (1997). *TNM Classification of Malignant Tumors* 5th edn. Wiley-Liss, Inc: New York, pp. 59–62.
Suzuki T, Yokozaki H, Kuniyasu H, Hayashi K, Naka K, Ono S, Ishikawa T, Tahara E and Yasui W. (2000). *Int. J. Cancer*, **88,** 992–997.
Tahara H, Kuniyasu H, Yokosaki H, Yasui W, Shay JW, Ide T and Tahara E. (1995). *Clin. Cancer Res.*, **1,** 1245–1251.
Van Heek NT, Meeker AK, Kern SE, Yeo CJ, Lillemoe KD, Cameron JL, Offerhaus GL, Hicks JL, Wilentz RE, Goggins MG, De Marzo AM, Hruban RH and Maitra A. (2002). *Am. J. Pathol.*, **161,** 1541–1547.
Yanagihara K, Seyama T, Tsumuraya M, Kamada N and Yokoro K. (1991). *Cancer Res.*, **51,** 381–386.
Yaremko ML, Recant WM and Westbrook CA. (1995). *Genes Chromosomes Cancer*, **13,** 186–191.
Yasui W, Tahara E, Tahara H, Fujimoto J, Naka K, Nakayama J, Ishikawa F, Ide T and Tahara E. (1999). *Jpn. J. Cancer Res.*, **90,** 589–595.
Yasui W, Tahara H, Tahara E, Fujimoto J, Nakayama J, Ishikawa F, Ide T and Tahara E. (1998). *Jpn. J. Cancer Res.*, **89,** 1099–1103.
Yasui W, Yokozaki H, Fujimoto J, Naka K, Kuniyasu H and Tahara E. (2000). *J. Gastroenterol.*, **35,** 111–115.
Yustein AS, Harper JC, Petroni GR, Cummings OW, Moskaluk CA and Powell SM. (1999). *Cancer Res.*, **59,** 1437–1441.
Zhou XZ and Lu KP. (2001). *Cell*, **107,** 347–359.

DNA methylation profiles of differentiated-type gastric carcinomas with distinct mucin phenotypes

Junichi Motoshita,[1] Naohide Oue,[1] Hirofumi Nakayama,[1] Kazuya Kuraoka,[1] Phyu Phyu Aung,[1] Kiyomi Taniyama,[2] Keisuke Matsusaki[3] and Wataru Yasui[1,4]

[1]Department of Molecular Pathology, Hiroshima University Graduate School of Biomedical Sciences, 1-2-3 Kasumi, Minami-ku, Hiroshima 734-8551; [2]Institute for Clinical Research, National Hospital Organization Kure Medical Center/Chugoku Cancer Center, 3-1 Aoyama-cho, Kure, Hiroshima 737-0023; and [3]Department of Surgery, Hofu Institute of Gastroenterology, 14-33 Ekiminami, Hofu, Yamaguchi 747-0801, Japan

(Received March 15, 2005/Revised May 25, 2005/Accepted June 2, 2005/Online publication August 15, 2005)

Gastric carcinomas (GC) are classified into four phenotypes according to mucin expression. Previous studies revealed the association of distinct genetic profiles in GC with mucin phenotypic expression; however, the roles of epigenetic changes, such as DNA methylation, are poorly understood. We examined whether the phenotypic expression of GC was associated with DNA methylation of *hMLH1*, *MGMT*, *p16^{INK4a}*, *RAR-beta* or *CDH1*. Expression of HGM, M-GGMC-1, MUC2, and CD10 was analyzed immunohistochemically in 33 advanced GC with differentiated histology. HGM was expressed in 14 (42.4%) cases, M-GGMC-1 in five (15.2%) cases, MUC2 in 15 (45.5%) cases and CD10 in 18 (54.5%) cases. DNA methylation was detected in five (15.2%) cases for *hMLH1*, 11 (33.3%) cases for *MGMT*, 13 (39.4%) cases for *p16^{INK4a}*, 17 (51.5%) cases for *RAR-beta* and 14 (42.4%) cases for *CDH1* by bisulfite-polymerase chain reaction and methylation-specific polymerase chain reaction. DNA methylation of *hMLH1* occurred more frequently in MUC2-negative GC than in MUC2-positive GC ($P = 0.0488$, Fisher's exact test). In contrast, *MGMT* was more frequently methylated in MUC2-positive GC than in MUC2-negative GC ($P = 0.0078$, Fisher's exact test). There was no correlation between gastric or intestinal-markers and methylation of the *p16^{INK4a}*, *RAR-beta* and *CDH1* genes. These results indicate that DNA methylation of specific genes, such as *hMLH1* and *MGMT*, may be involved partly in the distinct phenotypic expression of GC. (*Cancer Sci* 2005; 96: 474–479)

Gastric carcinoma (GC) is one of the most common malignancies worldwide. GC are often classified histologically into two major types: the differentiated and undifferentiated types described by Nakamura *et al.*[1] or the Lauren intestinal and diffuse types[2] based on glandular structure. Various genetic and epigenetic alterations are associated with GC; some are found in both the intestinal and diffuse types, whereas others are type specific.[3,4] It was previously reported that GC can be subdivided according to mucin expression into four phenotypes:[5–7] (i) gastric or foveolar phenotype (G type); (ii) intestinal phenotype (I type); (iii) intestinal and gastric mixed phenotype (GI type); and (iv) neither gastric nor intestinal phenotype (N type). Despite the usefulness of the Lauren classification, there are several variations of the intestinal-type GC described by Lauren. To better understand the development of GC at the molecular level, it is important to analyze molecular alterations in intestinal-type GC according to the mucin phenotype. Distinct genetic changes appear to be associated with I type and G type GC. *p53* mutations and allelic deletions of the adenomatous polyposis coli (*APC*) gene are detected more frequently in I type GC than in G type GC,[8–11] whereas microsatellite instability (MSI) is detected more frequently in G type GC than in I type GC.[10,12] We reported previously that alterations of *p73*, including loss of heterozygosity and abnormal expression, play important roles in the genesis of G type GC.[13]

Several lines of evidence suggest that changes in DNA methylation patterns, such as hypermethylation of CpG islands, are common changes in human cancers.[14] Hypermethylation of CpG islands in promoters is associated with silencing of some tumor-related genes.[15–17] We previously reported DNA methylation of the *hMLH1*,[18] *MGMT*,[19] *p16^{INK4a}*, *RAR-beta* and *CDH1*[20] genes. In contrast to the many studies of genetic alterations in G type and I type GC, epigenetic alterations in G type and I type GC are poorly understood. Associations between genetic and epigenetic alterations have been reported. DNA methylation of *hMLH1* is associated with MSI,[21,22] and DNA methylation of *MGMT* is associated with G to A mutations in the *K-ras*[23] and *p53*[24] genes. Because MSI occurs frequently in G type GC, it is possible that DNA methylation of *hMLH1* may occur frequently in G type GC. In fact, it has been reported that DNA hypermethylation of *hMLH1* occurs frequently in G type GC.[25] Because *p53* mutations are detected frequently in I type GC, it is possible that DNA methylation of *MGMT* occurs in I type GC. However, the association between DNA methylation and the mucin phenotypic expression of GC has been investigated only for *hMLH1*.

In the present study, we investigated the association between expression of gastric-type and intestinal-type markers and DNA methylation status of *hMLH1*, *MGMT*, *p16^{INK4a}*, *RAR-beta* and *CDH1* in differentiated-type GC.

Materials and Methods

Tissue samples

Thirty-three samples of differentiated-type GC from 33 patients were examined. All GC samples were not early GC

[4]To whom correspondence should be addressed.
E-mail: wyasui@hiroshima-u.ac.jp

© Japanese Cancer Association doi: 10.1111/j.1349-7006.2005.0074.x

but advanced GC, that had invaded beyond the muscularis propria.[26] Samples were obtained at time of surgery at Hiroshima University Hospital (Hiroshima, Japan) and affiliated hospitals. Tissue samples for molecular analyses were frozen immediately in liquid nitrogen and stored at −80°C until use. We confirmed microscopically that the tumor specimens consisted mainly of carcinoma tissue (> 50%). For immunohistochemical staining, tissues were fixed in 10% buffered-formalin and embedded in paraffin. Tumor staging was carried out according to the tumor-node-metastasis stage grouping.[27] Because written informed consent was not obtained, for strict privacy protection, all samples were dis-identified before analyzing DNA methylation status. This procedure is in accordance with the Ethical Guidelines for Human Genome/Gene Research enacted by the Japanese Government.

Phenotypic analysis of gastric carcinomas

Tissue sections (4 μm thick) were prepared from paraffin blocks, and representative sections were immunostained for human gastric mucin (HGM), M-GGMC-1, MUC2 and CD10. Immunostaining was by the immunoperoxidase technique with a Histofine Simple Stain Kit (Nichirei Biosciences, Tokyo, Japan). Deparaffinized tissue sections were immersed in methanol containing 3% hydrogen peroxide for 15 min to block endogenous peroxidase activity. Microwave pretreatment in citrate buffer was carried out for 15–30 min to retrieve the antigenicity. The sections were then incubated with antibodies against gastric-type markers HGM (NCL-HGM-45M1; Novocastra, Newcastle, UK; dilution 1:50) and M-GGMC-1 (HIK1083; Kanto Kagaku, Tokyo, Japan; dilution 1:50), and intestinal-type markers MUC2 (Ccp58; Santa Cruz Biotechnology, Santa Cruz, CA, USA; dilution 1:200) and CD10 (NCL-CD10-270; Novocastra; dilution 1:50), for 1.5 h at 37°C followed by incubation with the secondary antibody for 30 min. The immunocomplexes were visualized with 3,3′-diaminobenzidine. Sections were then counterstained with hematoxylin. GC were classified as G type, I type, GI type or N type. G type comprised those samples in which > 30% of the tumor cells were positive for gastric-type markers and showed little staining with intestinal-type markers. I type comprised those specimens in which > 30% of the tumor cells were positive for MUC2 or in which > 5% of the tumor cells were positive for CD10 and showed little staining with gastric-type markers. GC that showed positive staining for both gastric-type and intestinal-type markers were classified as GI type, and those that showed no staining with those markers were classified as N type.

Genomic DNA extraction and methylation analysis

To examine DNA methylation patterns in the 5′ CpG islands of the *hMLH1*, *MGMT*, *p16^{INK4a}*, *RAR-beta* and *CDH1* genes, we extracted genomic DNA with a genomic DNA purification kit (Promega, Madison, WI, USA) and treated the genomic DNA with sodium bisulfite, as described previously.[28] In brief, 2 μg of genomic DNA was denatured by treatment with NaOH and modified with 3 M sodium bisulfite for 16 h. DNA samples were purified with Wizard DNA purification resin (Promega), treated with NaOH, precipitated with ethanol and resuspended in 25 μL water. Aliquots (2 μL) were used as templates for methylation-specific polymerase chain reaction (MSP) amplification of the *MGMT*, *p16^{INK4a}*, *RAR-beta* and *CDH1* genes. MSP primers for *MGMT*, *p16^{INK4a}*, *RAR-beta* and *CDH1* were described previously.[28–30] For analysis of DNA methylation of *hMLH1*, we carried out bisulfite-polymerase chain reaction (PCR) followed by restriction digestion as described previously.[31] Primers and PCR conditions used for amplifying specific DNA fragments of various target genes are listed in Table 1. PCR products (15 μg) were loaded onto 8% non-denaturing polyacrylamide gels, stained with ethidium bromide and visualized under UV light. According to the corresponding literature, CpG island hypermethylation in the regions examined revealed good correlation with epigenetic silencing of the respective target genes.[31–35]

Statistical methods

Fisher's exact test was used for statistical analysis. *P*-values less than 0.05 were regarded as statistically significant.

Results

Association between gastric-type and intestinal-type markers and DNA methylation

We carried out immunohistochemical analysis of 33 advanced differentiated-type GC (Fig. 1). Of the 33 GC, expression of gastric and intestinal markers was detected in 14 (42.4%) cases for HGM, five (15.2%) cases for M-GGMC-1, 15 (45.5%) cases for MUC2 and 18 (54.5%) cases for CD10. Next, DNA methylation status was investigated. Representative data for bisulfite-PCR followed by restriction digestion of the *hMLH1* gene and MSP of the *MGMT*, *p16^{INK4a}*, *RAR-beta* and *CDH1* genes are shown in Fig. 2. Of the 33 GC, DNA hypermethylation was detected in five (15.2%) cases for *hMLH1*, 11 (33.3%) cases for *MGMT*, 13 (39.4%) cases for *p16^{INK4a}*, 17 (51.5%) cases for *RAR-beta* and 14 (42.4%) cases for *CDH1*. Although recent evidence suggests that methylation of certain genes such as *hMLH1* and *CDH1* is associated with aging,[36,37] there was no correlation between age and DNA methylation of a specific gene (Table 2). We compared DNA methylation status with each marker (Tables 3–6). DNA methylation of *hMLH1* was detected more frequently in MUC2-negative GC (5/18, 27.8%) than in MUC2-positive GC (0/15, 0.0%, $P = 0.0488$, Fisher's exact test). In contrast, DNA methylation of *MGMT* was detected more frequently in MUC2-positive GC (9/15, 60.0%) than in MUC2-negative GC (2/18, 11.1%, $P = 0.0078$, Fisher's exact test) (Table 5). There was no correlation between gastric and intestinal markers and methylation of the *p16^{INK4a}*, *RAR-beta* and *CDH1* genes.

Phenotypic expression of gastric carcinomas

On the basis of the combinations of expression of these four mucin markers, the 33 GC were classified phenotypically as five (15.2%) G type, 14 (42.4%) I type, 9 (27.2%) GI type and five (15.2%) N type. There was no apparent correlation between mucin phenotypic expression and clinicopathological findings (data not shown). No apparent association was observed between DNA methylation of a specific gene and phenotypic expression of GC (data not shown).

Table 1. Primer sequences for DNA methylation analysis

Primer sequence	Primer sequence	Annealing temperature
hMLH1		
	F: 5′-TAGTAGTYGTTTTAGGGAGGGA -3′ R: 5′-TCTAAATACTCAACRAAAATACCTT-3′	55°C
MGMT (unmethylated)		
	F: 5′-TTTGTGTTTTGATGTTTGTAGGTTTTTGT-3′ R: 5′-AACTCCACACTCTTCCAAAAACAAAACA-3′	59°C
MGMT (methylated)		
	F: 5′-TTTCGACGTTCGTAGGTTTTCGC-3′ R: 5′-GCACTCTTCCGAAAACGAAACG-3′	59°C
p16^{INK4a} (unmethylated)		
	F: 5′-TTATTAGAGGGTGGGGTGGATTGT-3′ R: 5′-CCACCTAAATCAACCTCCAACCA-3′	60°C
p16^{INK4a} (methylated)		
	F: 5′-TTATTAGAGGGTGGGGCGGATCGC-3′ R: 5′-CCACCTAAATCGACCTCCGACCG-3′	65°C
RAR-beta (unmethylated)		
	F: 5′-TTAGTAGTTTGGGTAGGGTTTATT -3′ R: 5′-CCAAATCCTACCCCAACA-3′	55°C
RAR-beta (methylated)		
	F: 5′-GGTTAGTAGTTCGGGTAGGGTTTATC-3′ R: 5′-CCGAATCCTACCCCGACG-3′	64°C
CDH1 (unmethylated)		
	F: 5′-TAATTTTAGGTTAGAGGGTTATTGT-3′ R: 5′-CACAACCAATCAACAACACA-3′	53°C
CDH1 (methylated)		
	F: 5′-TTAGGTTAGAGGGTTATCGCGT-3′ R: 5′-TAACTAAAAATTCACCTACCGAC-3′	57°C

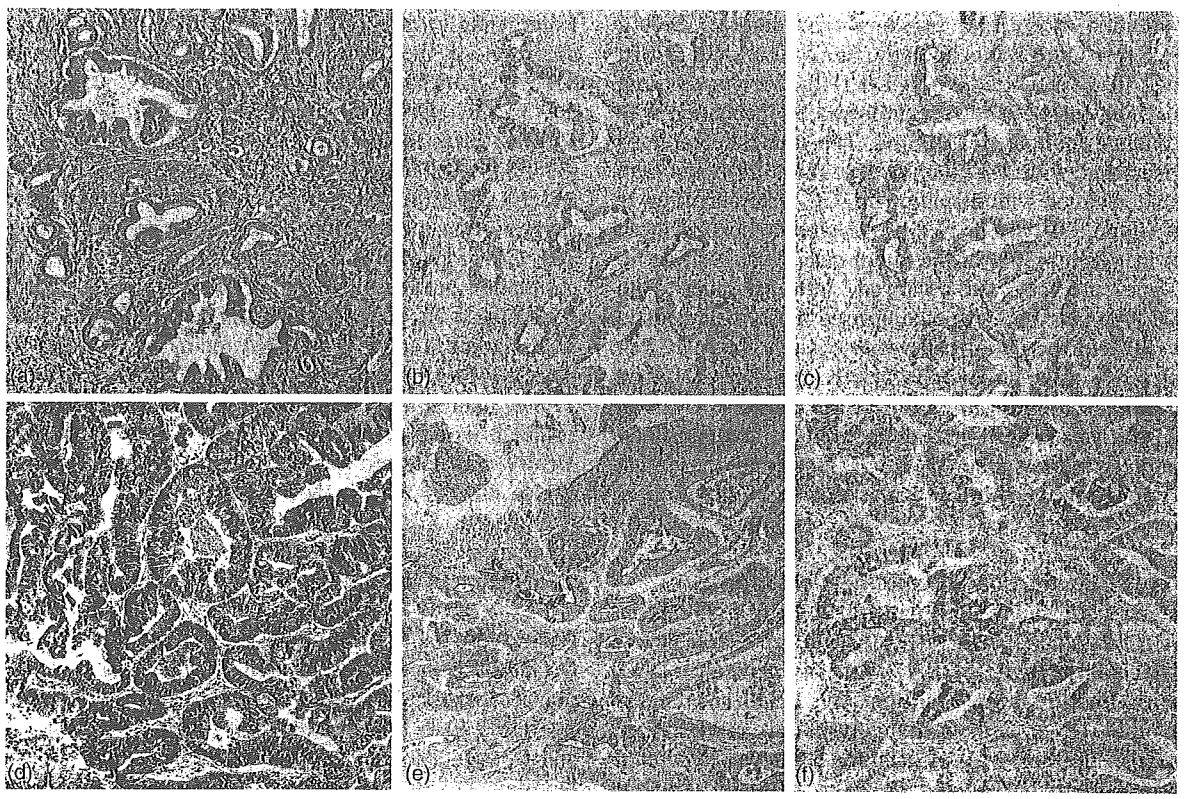

Fig. 1. G type (case 3: a, b, c) and I type (case 10: d, e, f) gastric carcinomas. (a,d) Hematoxylin and eosin staining. (b) MUC5AC and (c) M-GGMC-1 were detected in the cytoplasm of cancer cells. (e) CD10 was expressed on the luminal surfaces of cancer cells. (f) MUC2 is positive in the cytoplasm of cancer cells. (Original magnification, ×100).

© Japanese Cancer Association doi: 10.1111/j.1349-7006.2005.00074.x

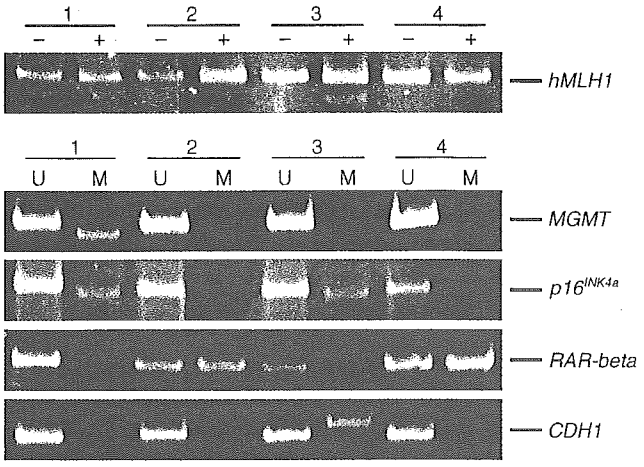

Fig. 2. Bisulfite-polymerase chain reaction followed by restriction digestion of the *hMLH1* gene and methylation-specific polymerase chain reaction of the *MGMT*, *p16*^{INK4a}, *CDH1* and *RAR-beta* genes. Methylated allele was detected in case 3 (*hMLH1*), case 1 (*MGMT*), cases 1 and 3 (*p16*^{INK4a}), cases 2 and 4 (*RAR-beta*) and case 3 (*CDH1*). M, methylated; U, unmethylated; +, after restriction enzyme digestion; –, before restriction enzyme digestion.

Table 2. Association between age and DNA methylation

Gene	Methylation status	Age		*P*-value†
		> 61	≤ 60	
hMLH1	Methylated	5 (100.0%)	0	0.5663
	Unmethylated	22 (78.6%)	6	
MGMT	Methylated	7 (63.6%)	4	0.1458
	Unmethylated	20 (90.9%)	2	
p16^{INK4a}	Methylated	11 (84.6%)	2	1.0000
	Unmethylated	16 (80.0%)	4	
RAR-beta	Methylated	13 (76.5%)	4	0.6562
	Unmethylated	14 (87.5%)	2	
CDH1	Methylated	11 (78.6%)	3	1.0000
	Unmethylated	16 (84.2%)	3	

†Fisher's exact test.

Table 3. Association between human gastric mucin (HGM) expression and DNA methylation status

Gene	Methylation status	HGM expression		*P*-value†
		Positive	Negative	
hMLH1	Methylated	2 (40.0%)	3	1.0000
	Unmethylated	12 (42.9%)	16	
MGMT	Methylated	5 (45.5%)	6	1.0000
	Unmethylated	9 (40.9%)	13	
p16^{INK4a}	Methylated	7 (53.8%)	6	0.4720
	Unmethylated	7 (35.0%)	13	
RAR-beta	Methylated	8 (47.1%)	9	0.7283
	Unmethylated	6 (37.5%)	10	
CDH1	Methylated	7 (50.0%)	7	0.4969
	Unmethylated	7 (36.8%)	12	

†Fisher's exact test.

Table 4. Association between M-GGMC-1 expression and DNA methylation status

Gene	Methylation status	M-GGMC-1 expression		*P*-value†
		Positive	Negative	
hMLH1	Methylated	1 (20.0%)	4	1.0000
	Unmethylated	4 (14.3%)	24	
MGMT	Methylated	1 (9.1%)	10	0.6431
	Unmethylated	4 (18.2%)	18	
p16^{INK4a}	Methylated	1 (7.7%)	12	0.6253
	Unmethylated	4 (20.0%)	16	
RAR-beta	Methylated	2 (11.8%)	15	0.6562
	Unmethylated	3 (18.8%)	13	
CDH1	Methylated	3 (21.4%)	11	0.6285
	Unmethylated	2 (10.5%)	17	

†Fisher's exact test.

Table 5. Association between MUC2 expression and DNA methylation status

Gene	Methylation status	MUC2 expression		*P*-value†
		Positive	Negative	
hMLH1	Methylated	0 (0.0%)	5	0.0488
	Unmethylated	15 (53.6%)	13	
MGMT	Methylated	9 (81.8%)	2	0.0078
	Unmethylated	6 (27.3%)	16	
p16^{INK4a}	Methylated	7 (53.8%)	6	0.4928
	Unmethylated	8 (40.0%)	12	
RAR-beta	Methylated	8 (47.1%)	9	1.0000
	Unmethylated	7 (43.8%)	9	
CDH1	Methylated	5 (35.7%)	9	0.4824
	Unmethylated	10 (52.6%)	9	

†Fisher's exact test.

Table 6. Association between CD10 expression and DNA methylation status

Gene	Methylation status	CD10 expression		*P*-value†
		Positive	Negative	
hMLH1	Methylated	1 (20.0%)	4	0.1523
	Unmethylated	17 (60.7%)	11	
MGMT	Methylated	8 (72.7%)	3	0.2659
	Unmethylated	10 (45.5%)	12	
p16^{INK4a}	Methylated	7 (53.8%)	6	0.7332
	Unmethylated	11 (5.0%)	9	
RAR-beta	Methylated	7 (41.2%)	10	0.1663
	Unmethylated	11 (68.8%)	5	
CDH1	Methylated	6 (42.9%)	8	0.3041
	Unmethylated	12 (63.2%)	7	

†Fisher's exact test.

Discussion

Gastric carcinomas are classified into the G, I, GI, and N phenotypes according to gastric-type and intestinal-type markers. In this study, expression of HGM, M-GGMC-1, MUC2 and CD10 was investigated. We observed that *hMLH1* was rarely methylated, whereas *MGMT* was frequently methylated in MUC2-positive GC. Therefore, DNA methylation, especially of the *hMLH1* and *MGMT* genes, may participate partly in the distinct phenotypic expression of GC. In fact, recent studies showed that the *MUC2* gene is also a target of DNA methylation.[38] Changes in genome-wide DNA methylation may also affect DNA methylation of these genes. To our knowledge, there is no report regarding DNA methylation of HGM, M-GGMC-1 and CD10.

DNA hypermethylation of *MGMT* occurred frequently in MUC2-positive GC. Previously reported data indicate that DNA hypermethylation of *MGMT* is associated with a G to A mutation in the *K-ras* and *p53* genes.[23,24] Although we found no association between DNA methylation of *MGMT* and I type GC, MUC2 is a marker of intestinal epithelial cells. Thus, frequent *p53* mutations in I type GC[8–11] may be due to DNA methylation of *MGMT*.

The *hMLH1* gene was rarely methylated in MUC2-positive GC in this study. Endoh *et al.* reported that DNA hypermethylation of *hMLH1* occurs frequently in G type GC,[25] which does not express MUC2. Our findings support the notion that DNA methylation of *hMLH1* occurs frequently in G type GC. On the other hand, MUC2-positive GC were reported to show MSI more frequently than MUC2-negative GC.[39] DNA methylation of *hMLH1* is associated with MSI, indicating that MUC2-positive GC may have frequent DNA methylation of *hMLH1*. The reason for the discrepancy between our results and those of Lee *et al.* is unclear; however, the discrepancy may be due to differences in the samples analyzed.[39] Lee *et al.* studied the MUC2 expression and MSI in both differentiated-type and undifferentiated-type GC, whereas we analyzed the phenotypic expression and DNA methylation in differentiated-type GC only. Taken together, MUC2-positive undifferentiated-type GC may show frequent MSI and DNA methylation of *hMLH1*. In addition, because of a phenotypic shift from G type to I type expression in conjunction with tumor progression,[7] G type early GC showing *hMLH1* methylation may lose G type expression along with tumor progression.

There was no correlation between mucin marker expression and DNA methylation of $p16^{INK4a}$, *CDH1* and *RAR-beta*. Hypermethylation of the $p16^{INK4a}$ gene is more common in differentiated-type GC than in undifferentiated-type GC, whereas *CDH1* and *RAR-beta* hypermethylation is observed more frequently in undifferentiated-scattered-type GC than in other types.[20] Thus, DNA methylation of these three genes may be involved in histogenesis, but not in phenotypic expression of GC.

Although MUC2 expression was correlated with DNA methylation of *hMLH1* and *MGMT* in this study, the number of cases we studied was too small to clarify correlation between phenotypic expression of GC and DNA methylation status. Additional studies are needed to obtain the definite association between DNA methylation and G and I phenotypes of GC.

In conclusion, our data show that DNA methylation of specific genes, such as *hMLH1* and *MGMT*, may be associated with the distinct phenotypic expression of GC. Because DNA methylation of tumor-related genes has been shown to occur in the early stages of stomach carcinogenesis[40] and to increase in parallel with stomach carcinogenesis,[41] the association between DNA methylation and GC phenotypes in early GC should be investigated.

Acknowledgments

We thank M. Takatani for excellent technical assistance and advice. This work was carried out with the kind cooperation of the Research Center for Molecular Medicine (RCMM), Faculty of Medicine, Hiroshima University. We thank the Analysis Center of Life Science, Hiroshima University, for the use of their facilities. This work was supported, in part, by Grants-in-Aid for Cancer Research from the Ministry of Education, Culture, Science, Sports, and Technology of Japan, and from the Ministry of Health, Labor, and Welfare of Japan.

References

1 Nakamura K, Sugano H, Takagi K. Carcinoma of the stomach in incipient phase: its histogenesis and histological appearances. *Gann* 1968; **59**: 251–8.
2 Lauren P. The two histological main types of gastric carcinoma. Diffuse and so-called intestinal type carcinoma: an attempt at histological classification. *Acta Pathol Microbiol Scand* 1965; **64**: 31–49.
3 Yasui W, Yokozaki H, Fujimoto J, Naka K, Kuniyasu H, Tahara E. Genetic and epigenetic alterations in multistep carcinogenesis of the stomach. *J Gastroenterol* 2000; **35**: 111–15.
4 Oue N, Hamai Y, Mitani Y *et al.* Gene expression profile of gastric carcinoma: identification of genes and tags potentially involved in invasion, metastasis, and carcinogenesis by serial analysis of gene expression. *Cancer Res* 2004; **64**: 2397–405.
5 Fiocca R, Villani L, Tenti P *et al.* Characterization of four main cell types in gastric cancer: foveolar, mucopeptic, intestinal columnar and goblet cells. An histopathologic, histochemical and ultrastructural study of 'early' and 'advanced' tumours. *Pathol Res Pract* 1987; **182**: 308–25.
6 Tatematsu M, Ichinose M, Miki K, Hasegawa R, Kato T, Ito N. Gastric and intestinal phenotypic expression of human stomach cancers as revealed by pepsinogen immunohistochemistry and mucin histochemistry. *Acta Pathol Jpn* 1990; **40**: 494–504.
7 Tatematsu M, Tsukamoto T, Inada K. Stem cells and gastric cancer: role of gastric and intestinal mixed intestinal metaplasia. *Cancer Sci* 2003; **94**: 135–41.
8 Uchino S, Noguchi M, Ochiai A, Saito T, Kobayashi M, Hirohashi S. p53 mutation in gastric cancer: a genetic model for carcinogenesis is common to gastric and colorectal cancer. *Int J Cancer* 1993; **54**: 759–64.
9 Kushima R, Muller W, Stolte M, Borchard F. Differential p53 protein expression in stomach adenomas of gastric and intestinal phenotypes. Possible sequences of p53 alteration in stomach carcinogenesis. *Virchows Arch* 1996; **428**: 223–7.
10 Endoh Y, Sakata K, Tamura G *et al.* Cellular phenotypes of differentiated-type adenocarcinomas and precancerous lesions of the stomach are dependent on the genetic pathways. *J Pathol* 2000; **191**: 257–63.
11 Wu LB, Kushima R, Borchard F, Molsberger G, Hattori T. Intramucosal carcinomas of the stomach: phenotypic expression and loss of heterozygosity at microsatellites linked to the APC gene. *Pathol Res Pract* 1998; **194**: 405–11.
12 Shibata N, Watari J, Fujiya M, Tanno S, Saitoh Y, Kohgo Y. Cell kinetics and genetic instabilities in differentiated type early gastric cancers with different mucin phenotype. *Hum Pathol* 2003; **34**: 32–40.
13 Yokozaki H, Shitara Y, Fujimoto J, Hiyama T, Yasui W, Tahara E. Alterations of p73 preferentially occur in gastric adenocarcinomas with foveolar epithelial phenotype. *Int J Cancer* 1999; **83**: 192–6.

© Japanese Cancer Association doi: 10.1111/j.1349-7006.2005.00074.x